The *mvp2* mutation affects the generative transition through the modification of transcriptome pattern, salicylic acid and cytokinin metabolism in *Triticum monococcum*

Ákos Boldizsár[1], Radomíra Vanková[2], Aliz Novák[1,3], Balázs Kalapos[1,3], Zsolt Gulyás[1,3], Magda Pál[1], Kristyna Floková[4], Tibor Janda[1], Gábor Galiba[1,5,*], Gábor Kocsy[1,3]

[1] Agricultural Institute, Centre for Agricultural Research, Hungarian Academy of Sciences, Martonvásár, 2462, Hungary

[2] Laboratory of Hormonal Regulations in Plants, Institute of Experimental Botany, Academy of Sciences of the Czech Republic, 165 02 Prague 6, Czech Republic

[3] Doctoral School of Molecular and Nanotechnologies, Research Institute of Chemical and Process Engineering, Faculty of Information Technology, University of Pannonia, Veszprém, 8200, Hungary

[4] Laboratory of Growth Regulators, Centre of the Region Haná for Biotechnological and Agricultural Research, Institute of Experimental Botany AS CR & Faculty of Science, Palacký University, CZ-78371 Olomouc, Czech Republic

[5] Doctoral School of Animal and Agricultural Environmental Sciences, Department of Meteorology and Water Management Georgikon Faculty, University of Pannonia, Keszthely, 8360, Hungary

[*]Corresponding author

Ákos Boldizsár	boldizsar.akos@agrar.mta.hu
Radomíra Vanková	vankova@ueb.cas.cz
Aliz Novák	novak.aliz@agrar.mta.hu
Balázs Kalapos	kalapos.balazs@agrar.mta.hu
Zsolt Gulyás	gulyas.zsolt@agrar.mta.hu
Magda Pál	pal.magda@agrar.mta.hu
Kristyna Floková	kristyna.flokova@yahoo.fr
Gábor Galiba	galiba.gabor@agrar.mta.hu
Tibor Janda	janda.tibor@agrar.mta.hu
Gábor Kocsy	kocsy.gabor@agrar.mta.hu

1 Summary

Wild type and *mvp2* (maintained vegetative phase) deletion mutant *T. monococcum* plants incapable of flowering were compared in order to determine the effect of the deleted region of chromosome 5A on transcript profile and hormone metabolism. This region contains the vernalization1 (*VRN1*) gene, a major regulator of the vegetative/generative transition. Transcript profiling in the crowns of *T. monococcum* during the transition and the subsequent formation of flower primordia showed that 306 genes were affected by the mutation, 198 by the developmental phase and 14 by the interaction of these parameters. In addition, 546 genes were affected by two or three factors. The genes controlled by the deleted region encode transcription factors, antioxidants and enzymes of hormone, carbohydrate and amino acid metabolism. The observed changes in the expression of the gene encoding phenylalanine ammonia lyase (*PAL)* indicated the effect of *mvp2* mutation on the metabolism of salicylic acid, which was also corroborated by the differences in 2-hydroxycinnamic acid and cinnamic acid contents in both of the leaves and crowns, and in the concentrations of salicylic acid and benzoic acid in crowns during the vegetative/generative transition. The amount and ratio of active cytokinins and their derivatives (ribosides, glucosides and phosphates) were affected by developmental changes as well as by *mvp2* mutation, too. The absence of *VRN1* and other neighbouring genes in the *mvp2* mutant plants resulted in the modification of the transcriptome, salicylic acid and cytokinin levels, which changes contributed to the continuous maintenance of the vegetative phase.

2 Keywords

cytokinin, *mvp2* mutation, *Triticum monococcum*, vegetative/generative transition, vernalization

3 Abbreviations

Genotypes:

Tm wt or wt: *Triticum monococcum* wild type; *mvp2*: *Triticum monococcum* maintained vegetative phase mutant;

Salicylic acid metabolism:

CA: cinnamate; *o*HCA: 2-hydroxy-cinnamic acid (*ortho*-hydroxy-cinnamic acid); BA: benzoate; SA: salicylate;

Light conditions:

Ppd: photoperiod response gene; SD: short day; LD: long day;

Development:

VP 20 °C: vegetative phase at 20 °C, single ridge structure of the apices; VP 4 °C: vegetative phase at 4 °C; DR: double ridge, this phenophase shows the vegetative/generative transition during the development; SI: initiation of spike primordia;

Cytokinins:

CK: cytokinin; tZ: *trans*-zeatin; DHZ: dihydrozeatin; iP: isopentenyladenine; cZ: *cis*-zeatin; tZR: *trans*-zeatin riboside; DHZR: dihydrozeatin riboside; iPR: isopentenyladenosine; cZR: cZ riboside; tZR5'MP: tZR 5'- monophosphate; DHZR5'MP: DHZR 5'-monophosphate; iPR5'MP: iPR 5'-monophosphate; cZR5'MP: cZR 5'-monophosphate; tZ9G: tZ-N9-glucoside; DHZ9G: DHZ-N9-glucoside; iP9G: iP-N9-glucoside; cZ9G: cZ-N9-glucoside; tZOG: tZ-O-glucoside; tZROG: tZR-O-glucoside; DHZOG: DHZ-O-glucoside; DHZROG: DHZR-O-glucoside; cZOG: cZ-O-glucoside; cZROG: cZR-O-glucoside

4 Introduction

The exact flowering time is of key importance for perennial grasses since their reproductive organs are highly sensitive to low temperature. Winter wheat necessitates an exposure to low temperature to fulfil its vernalization requirement and ensure its transition from the vegetative to the reproductive phase. Without cold treatment, winter wheat genotypes are incapable of flowering, while spring genotypes do not have such demands. If the transition to the generative phase occurs too early, even a milder frost may result in great yield loss due to the considerable decrease of freezing tolerance.

Flowering time is controlled by three well characterized gene families (Laurie, 1997). Photoperiod response genes (*Ppd*) sense day length, and usually, long day (LD) conditions induce their expression. The second gene family contains 'earliness *per se*' factors, which take part in the initiation of floral primordia and in the determination of the numbers of vegetative and generative primordia independently of environmental conditions (Worland, 1996). The third family consists of the vernalization genes *VRN1*, *VRN2* and *VRN3*, which are inducible by low temperature. Their allelic differences and interactions are important in the timing of the vegetative/generative transition (see for review Distelfeld et al. 2009; Galiba et al. 2009). During vernalization at low temperature, *VRN1* is induced, which inhibits the flowering repressor, *VRN2*. In consequence, the inhibition imposed by *VRN2* on *VRN3*, an activator of flowering, is terminated, and the vegetative/generative transition occurs. The role of *VRN1* region in the induction of flowering was demonstrated by using maintained

vegetative phase (*mvp2*) mutant that never flowers (Shitsukawa et al., 2007b). The effect of *mvp2* mutation on transcriptome was investigated after one week cold period when the seedlings were still in the double ridge stage (Diallo et al., 2014). Genes related to transcriptional regulation, sugar metabolism, oxidative and biotic stresses were affected by the mutation. However, no transcriptomic data are available during the formation of spikelet primordia. Detail analysis revealed that besides the *VRN1* gene, the *AGAMOUS-LIKE GENE 1* [*AGLG1;* control of fruit development (Yan et al., 2003)], the *CYSTEINE PROTEINASE (CYS;* degradation of proteins) and *PHYTOCHROME-C (PHY-C)* genes were also deleted in the *mvp2* mutant. The latter gene encodes a photoreceptor that affects also flowering in a light-dependent way (Chen et al., 2014; Distelfeld and Dubcovsky, 2010).

Besides the above mentioned major regulators of vernalization, the expression of a large gene set changes during the induction of this process by low temperature as shown by transcriptome analysis in wheat (Gulick et al., 2005; Majláth et al., 2012; Monroy et al., 2007; Winfield et al., 2009). Comparison of the transcriptome profile in a spring and winter wheat genotype during cold treatment showed different expression of genes encoding among others protein kinases, putative transcription factors and Ca-binding proteins (Gulick et al., 2005). Winfield et al. (2009) monitored the developmental-phase-dependent gene expression changes and identified several MADS-box genes, which may play an important role in the onset of flowering. The investigation of cold-induced transcript profile changes in chromosome 5A substitution lines ensured the possibility of obtaining more information about the control of flowering since the *VRN1* gene is localised on this chromosome. The alterations of the transcriptome of plants in vegetative stage have been compared in winter and spring line, and expression of the gene encoding *Dem* (deficient embryo and meristem) protein affecting the development of apical meristem was proved to be different (Kocsy et al., 2010).

Plant growth regulators, especially gibberellins (Mutasa-Gottgens and Hedden, 2009), play an important role in the control of flowering. The auxins also regulate flowering through the members of the AINTEGUMENTA-LIKE/PLETHORA transcription factor family (Krizek, 2011). The role of methyl jasmonate in this process was recently shown in *T. monococcum*, where its level was higher, and many jasmonate-responsive genes were affected in non-flowering *mvp2* mutant (Diallo et al., 2014). In addition, treatment with this hormone delayed flowering with simultaneous downregulation of *VRN1* and *VRN3* genes. Moreover, salicylic acid (SA) participates also in the control of flowering time since SA-deficient plants flower later and UV-C stress activates the vegetative/generative transition in *Arabidopsis* through

this hormone (Martínez et al., 2004). The involvement of cytokinins as a long-distance signal of the floral transition process has also been recently shown (Bernier, 2013). Transient cytokinin maximum was observed at the onset of vegetative-generative transition both in *Brassica napus* (Tarkowská et al., 2012) and *Triticum monococcum* (Vanková et al., 2014).

Despite the intensive study of the regulation of flowering processes, the transcriptional and hormonal control during the initial development of flower primordia in wheat plant is still poorly understood. In the present experiments the possible involvement of the *mvp2* mutation-dependent changes of transcriptome profile and the SA and cytokinin metabolism in the control of vegetative/generative transition have been studied.

5 Materials and methods

5.1 Plant material and treatments

Triticum monococcum KU 104-1 strain and its *mvp2* mutant were analysed in this study. The *mvp2* mutant was generated by ion beam radiation and has a large deletion that includes *VRN1* (Shitsukawa et al., 2007b) and the other three genes (Distelfeld and Dubcovsky, 2010).

After germination in Petri dishes between wet filter papers (1 d 25 °C, 3 d 5 °C, 2 d 25 °C), seedlings were grown with a photoperiod of 16 h (light cycle started at 2:00 and finished at 18:00), at 260 µmol m^{-2} s^{-1}, 20/17 °C and 75/65% RH in a growth chamber (Conviron PGV-15; Controlled Env., Ltd., Winnipeg, Canada). Seedlings were raised in a 2:1:1 (V/V/V) mixture of garden soil, humus and sand in wooden boxes (150 plants in a box). Dimensions of the soil blocks in the boxes were 26 × 38 × 10 cm (length × width × depth), distance between the plants was 2.5 cm. After 3 weeks, temperature was set immediately to continuous 4 °C (day/night), other environmental parameters remained unchanged. Crown and leaf (the second youngest leaves) samples were taken for hormone measurements (in case of cytokinin analysis, only the leaves were examined) and gene expression studies before the cold treatment; after 2 weeks at 4 °C, when the seedlings were still in the vegetative developmental stage; during the vegetative/generative transition (double ridge stage) and after the appearance of the spikelet primordia (spikelet initiation phase). In the last two sampling points samples for microarray analysis were collected separately from the crowns. Although there was no developmental phase change in *mvp2*, the samples from this genotype were collected at the same time as in the wild type and the same nomenclature was used for the indication of the sampling points (Fig. 1). Each sampling was started after a 6-hour illumination and lasted for 60-90 min. The experiments were repeated 3 times. In each experiment, 3 samples consisting of a mixture of the crowns and leaves, respectively, from 9 plants were analysed.

5.2 Selection of the *mvp2* mutants by genotyping

Leaf samples (100 mg FW) were collected from the seedlings and disrupted by TissueLyser (Qiagen) (shaking settings: 25 Hz, 90 sec). The total DNA was isolated from crushed material by the Zeno-Gene40 DNA isolation kit (Zenon Bio Ltd.) and eluted in 200 µl of elution buffer in the last step. Genotyping was carried out in two-steps. In the first screening step a 1084 bp long segment of the *VRN1* gene was amplified by PCR (Applied Biosystems® GeneAmp® PCR System 9700) according to the manufacturer's instructions. The reaction mixture contained 2.5 µl 10x Key buffer, 2.5 µl DNA, 0.5-0.5 µl VRN1-specific primers (10 µM , Suppl. table 1), 0.5 µl dNTP mix (2.5 mM), 0.4 µl Red Taq enzyme (Red Taq DNA Polymerase enzyme (VWR)) and 18.1 µl water. The chosen primers amplified the fragment of the *VRN1* gene not present in the homozygous mutant. The applied PCR conditions were as follows: 40 cycles of 94 °C for 20 sec, 61 °C for 30 sec, and 72 °C for 80 sec. In case of ambiguous samples, the second screening step was employed. According to Dhillon et al. (2010) a modified method was applied. The following primers were used in 10 µM concentration: 1 µl F18, 0.5 µl R23 and 0.75 µl R22. In this multiplex PCR reaction the wild type *Triticum monococcum* gives two amplicons (172 and 339 bp) while *mvp2* mutant gives only one amplicon. The sequence of the primers is given in the Suppl. table S1.

5.3 Selection of the sampling time according to the morphology of shoot apices

The developmental stage of the shoot apices, isolated from the crowns of the seedlings, was determined under a Zeiss Stemi 2000-C stereomicroscope (Carl Zeiss Mikroskopie, Jena, Germany) according to the scale of Gardner (Gardner et al., 2007) (Fig. 1). Three developmental phases were distinguished according to the wild type: vegetative (VP, single ridge structure, Gardner's stages 0-1), double ridge (DR, vegetative/generative transition, Gardner's stage 3) and generative phases (SI, initiation of spike primordia, Gardner's stages 4-5).

5.4 Determination of hormones

Methanol-soluble free and bound SA and their precursors were measured according to Pál et al. (2005), who modified the method of Meuwly and Métraux (1993). Benzoic acid (BA) and cinnamic acid (CA) were measured by UV spectrophotometry in the range of 230–300 nm (W996 photodiode array detector, Waters, Milford, MA). SA and *ortho*-hydroxy-cinnamic acid (*o*HCA) were quantified fluorimetrically (W474 scanning fluorescence detector), with excitation at 317 nm and emission at 436 nm for *o*HCA, followed by excitation at 305 nm and emission at 407 nm for SA.

Cytokinins were extracted and purified as described earlier (Svačinova et al., 2012), with modifications. Briefly, 1ml $2*10^{-8}$ M concentration of ice cold extraction mixture of methanol/water/formic acid (15/4/1, V/V/V) containing stable-isotope-labelled internal standards of cytokinins ($^2H_5$-tZ, $^2H_5$-tZR, $^2H_5$-tZRMP, $^2H_5$-tZ7G, $^2H_5$-tZ9G, $^2H_5$-tZOG, $^2H_5$-tZROG, $^2H_3$-DZ, $^2H_3$-DZR, $^2H_3$-DZRMP, $^2H_3$-DZ9G, $^2H_7$-DZOG, $^2H_6$-iP, $^2H_6$-iPR, $^2H_6$-iPRMP, $^2H_6$-iP7G, $^2H_6$-iP9G) was added to homogenized samples and stirred for 30 min/4˚C. After centrifugation the supernatants were passed through the Sep-Pak Plus C_{18} cartridge (Waters, Milford, MA, USA) to remove the lipids and pigments. Cytokinins from flow-through fraction were concentrated by mixed mode Oasis MCX reverse phase-cation exchange SPE column (Waters, Milford, MA, USA) and eluted with 0.35 M NH_4OH in 60% methanol. Eluates were evaporated to dryness in a Speed-Vac concentrator RC1010 (Jouan, Winchester, UK) and reconstituted by 30 µl of mobile phase prior to UHPLC-MS/MS analysis. An Acquity UPLC® System (Waters, Milford, MA, USA) coupled to a triple quadrupole mass spectrometer Xevo™ TQ MS (Waters MS Technologies, Manchester, UK) with an electrospray interface (ESI) was employed in cytokinin analysis. Compounds were separated on reverse-phase column (Acquity UPLC® BEH C18, 1.7 µm, 2.1 × 150 mm, Waters) by 24 min binary gradient consisting of methanol (A) and 15 mM ammonium formate pH 4.0 (B) (Svačinova et al., 2012). The effluent was introduced in the ESI source of the tandem mass spectrometer Xevo TQ MS. Cytokinins were determined and quantified by multiple ion monitoring mode (MRM). MassLynx™ software (version 4.1, Waters, Milford, MA, USA) was used to operate the instrument, acquire and process the MS data.

5.5 Gene expression studies

Total RNA was isolated using Direct-zol™ RNA Miniprep Kit (Zymo Research) as described by the manufacturer. Reverse transcription was carried out with M-MLV reverse transcriptase and Oligo$(dT)_{18}$ primer (Thermo Scientific) according to the method of the supplier. 1500 ng RNA was transcribed into cDNA in 100 µl final volume. From this cDNA solution, 1 or 1.5 µl were utilized for the qRT-PCR analysis. Transcript levels were determined by real-time RT-PCR using a CFX96 Touch™ Real-Time PCR Detection System (Bio-Rad). Most primer sequences were designed by our group while those of *VRN1* were found in the literature (Loukoianov et al., 2005), (Suppl. table S1). In case of all primers, the efficiency ranged between 95 and 100%. Relative transcript levels were calculated by $\triangle\triangle C_t$ method using the housekeeping gene similar to phosphoglucanate dehydrogenase protein (unigene identifier: Ta30797) for normalization (Paolacci et al., 2009). In all cases the expression levels were compared to the DR phase of *Triticum monococcum* wild type (Tm wt). The Bio-Rad CFX

Manager 3.1 (File version: 3.1.1517.0823) calculated the relative normalized expression. In the charts, the error bars show the standard deviation and the y-axis was scaled in $\log_2$. The outliers were excluded from the analysis in case the standard deviation of C_t value exceeded 0.3 in the replicate group.

5.6 Microarray experiments

For microarray analysis, total RNA was isolated using Qiagen kit (RNeasy Plant Mini Kit). Three parallel samples were isolated from the crowns of Tm wt and mutant plants. 4000 ng total RNA samples were eluted in 40 µl final volume (100 ng/µl). 300 ng were analysed on gel and 200 ng were analysed with Agilent Bioanalyzer Instrument. RNA purity was checked by the absorbance ratios of 260/280 and 260/230 nanometres. Ratio of sample absorbance was 2 or higher. Gel electrophoresis confirmed the intactness of the RNAs. Samples with an RNA integrity number (RIN) above 8.0 were used for further analysis.

Total RNA (200 ng) was labelled and amplified using Low Input Quick Amp Labelling Kit according to the instructions of the manufacturer (Agilent Technologies). Labelled RNA was purified and hybridized to Agilent Wheat genome 4x44K array slides according to the manufacturer's protocol. After washing, array scanning and feature extraction were performed with default scenario by Agilent DNA Microarray Scanner. Fluorescence intensities of spots were quantified, background subtracted, and dye-normalized by Feature Extraction software, version 9.5 (Agilent Technologies). Data were then imported and analysed using GeneSpring GX program (Agilent Technologies) to generate lists of genes with a minimum 2-fold difference in the expression. Array data are available in ArrayExpress data bank with the ID E-MTAB-3968.

5.7 Statistical analysis

For the statistical analysis one-way ANOVA and Dunett t or Tukey B *post hoc* tests were used by SPSS 16.0. Normality was tested by Kolmogorov-Smirnov probe, homogeneity of the variances was tested by Levene's test.

6 Theory

The deletion in *mvp2* mutants including the *VRN1* gene is assumed to control the transcript profile changes during the vegetative/generative transition and initial development of the flower primordia. The alterations in gene expression may affect, among others, the metabolism of SA and cytokinins, i.e. hormones influencing flowering.

7 Results

7.1 Effect of the gene deletion and developmental stage on transcript profile

Based on selection criteria of a minimum 2-fold difference in the expression related to the genotype, developmental stage or their interactions, 1064 were selected from the 43604 genes present on the array (Suppl. Table 2). Comparison of transcript profiles in crowns of wild type and *mvp2* mutant plants during the vegetative/generative transition and the formation of spikelet primordia (Fig. 1) indicated that 198 genes were affected by the developmental phase, 306 by the *mvp2* mutation and 14 by their interactions (Fig. 2). In addition, 546 genes were affected by two or three factors.

7.2 Validation of microarray results and clustering of the selected genes

Microarray data allowed selecting several cold acclimation- or vegetative/generative transition-related genes that were differentially expressed in the crowns of the two genotypes or during the development. Microarray results were validated by qRT-PCR (Fig. 3). There was a close correlation (R^2=0.98) between the microarray and qRT-PCR results (Suppl. Fig. S1). The expression of *CBF4*, *CBF14* and *R2R3-MYB* genes exhibited a strong induction in wt plants between the DR and SI phases while it was constitutively high in the *mvp2* mutant (Figs. 3 A-C). The transcript level of *VRN1* decreased after the vegetative/generative transition in wt while it was not detectable in *mvp2* because of the deletion on the 5A chromosome (Fig. 3 D). The expression of the genes encoding a Ser-Thr protein kinase (*STPK*), *LG* (lipoxygenase), *C2H2* Zn-finger and heat shock proteins (*HSP17*, *HSP80*, *HSP101*) and *MPBF1* (multiprotein bridging factor 1) decreased in wt after entering the generative phase while it exhibited a continuously low level during both DR and SI phases in the mutant (Fig. 3 E-K). In case of *PAL* (phenylalanine ammonia-lyase), a lower decrease was observed in the *mvp2* plants in SI compared to the DR phase (Fig. 3 L). Changes in the expression of heat shock proteins (*HSP80*, *HSP17* and *HSP101*) showed similar tendencies. In the wild type, strong decrease was observed after the vegetative/generative transition and in *mvp2,* low transcript levels occurred at the DR phase which further decreased at SI phase (Fig. 3 H-J).

The pool of 1064 genes (in Fig. 2) was further filtered by ignoring those that were functionally not annotated and whose E-values were smaller than 1e-40. Two hundred genes satisfied these criteria (Suppl. Table 2). Relative expression values of wt SI, *mvp2* DR and *mvp2* SI normalised to wt DR were compared by hierarchical clustering. This revealed the genotype-dependency of genes related to stress tolerance and showed that genes related to

transcriptional regulation and carbohydrate metabolism were influenced by the developmental phase (Suppl. Fig. S2). After an additional selection, a filtered heat-map was constructed (Fig. 4) in which only those 137 genes were kept that exhibited more than 2-fold differences between the genotypes at DR phase (Fig. 4). Approximately one fourth of these genes showed higher expression in *mvp2* at the DR stage compared to the same developmental phase of wt, which may indicate their repression by one of the deleted genes (*VRN1, AGLG1, CYS* and *PHY-C*). Among these genes, several *CBF* and MADS-box transcription factors can be found. In contrast, many HSPs had greater expression in wt, which indicates their induction by the deleted gene(s).

7.3 Assignment of genotype- and development-responsive genes to biological processes, molecular functions, KEGG pathways and their networks

Different methods were chosen for evaluating the results of the microarray analysis (Suppl. Table 2). First of all, *Arabidopsis* homologs were selected whose E-value ≤ 1e-40 and whose expression differences between the compared groups (D, G, and common set of D × G) were higher than or equal to 2 (in $\log_2$ value). After that the genes were analysed by BiNGO Cytoscape plug-in software (Maere et al., 2005) to determine over-represented biological processes or molecular function categories. According to the categorization of biological processes, the first five groups containing the highest number of the genes influenced by the genotype are the metabolic process (GO:8152), primary metabolic process (GO:44238), response to stimulus (GO:50896), response to stress (GO:6950) and biosynthetic process (GO:9058), which contain 22, 19, 16, 15 and 12 genes, respectively (Suppl. Fig. 3). Two of these groups [response to stimulus (GO:50896), response to stress (GO:6950)] contain high number of genes influenced by the developmental phase, too. The following groups containing 7 and 6 genes influenced by D are the response to chemical stimulus (GO:42221) and response to abiotic stimulus (GO:9628), respectively. This indicates that, in our experiment, cold treatment was at least as effective on the gene expression changes as mutation. *PAL* is one of these genes, which prompted us to determine the SA content and investigate the SA biosynthesis in more detail.

Three molecular function GO categories contain most of the genes from the array: namely, catalytic activity (GO: 3824), oxidoreductase activity (GO:16491) and binding (GO:5488). The first category consists of 34 genes influenced by genotype and 18 influenced by developmental phase, while the second one contains 14 and 6 genes, respectively (Suppl. Fig. 4). Among the genes of the GO: 3824 category influenced by the genotype, the following two have the best E-values: glutamine-dependent asparagine synthetase (AAU89392.1) and

spermidine synthase (AHJ14572.1). Both genes are important in stress tolerance. Asparagine synthetase is essential in the synthesis of L-glutamate, the precursor of glutathione and spermidine. Spermidine synthase catalyses formation of spermidine enhancing tolerance against various stresses (Kasukabe et al., 2004). Interestingly, both genes had lower expression level in the *mvp2* genotype compared to wild type (Fig. 4 and Suppl. Fig 2). Among the identified oxidoreductase enzymes (GO:16491) ABA 8'-hydroxylase, the key enzyme in the catabolism of the abscisic acid (Krochko et al., 1998), had slightly lower activity (-0.25-fold difference) in the mutant genotype (Suppl. Fig. 2 and 4).

According to the KEGG pathway cluster analysis the main pathways containing the majority of genes influenced by genotype are general metabolic and secondary metabolites biosynthesis pathways followed by the steroid biosynthesis (ATH00100), phenylpropanoid biosynthesis (ATH00940) and phenylalanine metabolism (ATH00360) (Suppl. Fig. 5). The occurrence of the phenylalanine metabolism among the overrepresented KEGG pathways confirmed importance of the thorough examination of SA biosynthesis in order to determine the differences between the genotypes. However, the thorough analysis of the other processes (such as steroid biosynthesis and phenylpropanoid biosynthesis) exceeds the scope of this study.

Fig 5. shows the network of proteins encoded by the selected 59 genes (Suppl. Table 2 row C). Additional proteins interconnecting the former ones with proteins encoded by the four deleted genes were included. Protein-protein interactions were identified using the BioGRID (Oughtred et al., 2016) database, and were visualised by Osprey software (Breitkreutz et al., 2003). Gene selection was based on the homology between the *Triticum aestivum* and *Arabidopsis*. The deleted genes in *mvp2* were very close to each other (Yan et al., 2003). In wt *VRN1* and *AGLG1,* genes are next to each other and the other two genes are also localized close to *Vrn1* locus. In our map, instead of *AGLG, SEP4* and, instead of *CYS, SAG12* genes are presented because of the better E-values of the annotated sequences. In this network, three of the four deleted genes form a close linkage. From among the closest genes, 6 were present on the array and three of them, *AGL14, AGL20* (similar to *SOC1*) and *AGL19,* were induced because of the lack of *VRN1* (synonym name: *AP1), SEP4* and *SAG12. SOC1* (suppressor of overexpression of *CO1*) gene causes delayed flowering, according to the examination of mutant *Arabidopsis* (Onouchi et al., 2000), and it was determined in wheat that *WSOC1* acts upstream of *WAP1* (*wheat AP1 = VRN1*) or regulates the flowering in a different pathway from the *WAP1* (Shitsukawa et al., 2007b). In *Arabidopsis* there are three flowering regulatory pathways (long-day-, vernalization- and autonomous flowering pathways). *SOC1* is

connected to the first one, but these pathways are partially redundant. The expression of this gene is highly induced in the mutants that never flowers (Fig. 5). Our results are in accordance with the reports of Shitsukawa et al. (2007a, 2007b).

7.4 Effect of *mvp2* mutation and developmental stage on SA and cytokinin levels

SA can be synthesized in three different ways; besides SA itself, three of its possible precursors, cinnamic acid (CA), 2-hydroxy-cinnamic acid (*o*HCA) and benzoic acid (BA), were measured in the crowns and leaves of the wt and mutant plants before and after a two-week treatment at 4 °C, at the DR and SI stages (Fig. 6). The bound forms of all compounds were present in a much higher concentration than the free forms both in the crowns and leaves. In *mvp2* crowns at the VP at 20 °C, free *o*HCA, free BA and free SA were not present in detectable concentrations (Fig. 6 A, G and E). Exposure to low temperature increased the *o*HCA levels in the leaves and crowns, BA in the leaves in both genotypes, the levels of SA in the leaves and CA in the crowns in the mutant plants. At DR phase the bound forms of all measured compounds in the crowns were present in higher concentrations in the *mvp2* mutant than in wt plants (Fig. 6 A, C, E, G). Similar differences were observed in the leaves for *o*HCA and CA (Fig. 6 B and D). The differences between the genotypes were eliminated after the transition to the generative phase at SI. There were no alterations either in the crowns or in the leaves except in case of SA and CA in crowns where the amounts of free forms were greater in the mutant plants (Fig. 6 C and E).

Contents of cytokinin metabolites were compared in wt and *mvp2* leaves during the prolonged cold exposure associated in wt with developmental transition. General response of both genotypes to low temperature was down-regulation of the levels of precursors of active cytokinins, i.e. cytokinin phosphates (Suppl. Fig. 7C), which indicated suppression of cytokinin biosynthesis under non-optimal temperature. Physiologically the most active cytokinin is *trans*-zeatin. The biosynthesis of this cytokinin, presented according to the KEGG database, is shown in Suppl. Fig. 6 where all determined cytokinin metabolites are highlighted. Its isomer, *cis*-zeatin, which prevails in some monocots, is less active in the stimulation of cell division (by more than one order of magnitude), but maintains other CK functions and seems to be associated with stress responses. Apart of *trans*-zeatin and *cis*-zeatin, active cytokinins include also isopentenyladenine and dihydrozeatin (Suppl. Fig. 7A). The corresponding ribosides were reported to be predominantly transport forms (Lomin et al., 2015). Two-week long cold treatment had positive effect on *trans*-zeatin and its riboside in wt. In case of the mutant, low temperature resulted in decrease of isopentenyladenine, dihydrozeatin and *cis*-zeatin, while *trans*-zeatin riboside and isopentenyladenosine increased

(Fig. 7). The maximum of active cytokinins were found at the DR stage, i.e. during vegetative/generative transition. In wt, the predominant cytokinin was *trans*-zeatin, in mutant, *trans*-zeatin riboside and isopentenyladenosine prevailed. SI stage was associated with substantial drop of active cytokinins, especially in wt, which undertook successful developmental transition. Mutant preserved higher levels of isopentenyladenosine. The mutant constitutively remaining in vegetative stage exhibited decreased levels of cytokinin deactivation products – cytokinin N- and O-glucosides, especially of *trans*-zeatin-N9-glucoside, dihydrozeatin-N9-glucoside, *cis*-zeatin-N9-glucoside, *trans*-zeatin-O-glucoside, *cis*-zeatin-O-glucoside (Fig. 7). This may indicate diminished cytokinin biosynthesis or much slower turn-over of active cytokinins. In wt, concentration of cytokinin N- and O-glucosides exhibited a transient increase during DR, and then it decreased (Suppl. Figs. 7 D, E).

Thus, as shown in Suppl. Fig. 7, highly significant changes of cytokinins were observed during the vegetative/generative transition. Developmental phase affected content of *trans*-zeatin associated with stimulation of cell division. Precise regulation of active cytokinin levels is reflected by elevation of *trans*-zeatin-riboside, *trans*-zeatin O-glucoside, *trans*-zeatin N-glucoside, *cis*-zeatin O-glucoside.

8 Discussion

8.1 Effect of *mvp2* mutation and generative transition on the gene expression

The transcriptome analysis confirmed our hypothesis that *mvp2* mutation affects the vegetative/generative transition through the modification of the transcriptome profile since the expression of 306 gene differed in the mutant compared to the wild type plants. Several genes encoding agamous-like (AGL) MADS box transcription factors are possibly under the negative control of the protein encoded by one of the deleted genes as it was shown by their greater expression in the mutant. Based on our network of the proposed protein interactions (Fig. 5), the negative regulator is probably the VRN1 (AP1) protein that connects to several AGL proteins and is a major regulator of flowering. These AGL transcription factors control flowering at several levels including the timing of the generative transition and determination of floral meristem identity (Lee et al., 2000; Winfield et al., 2009; Yu et al., 2002). The freezing tolerance-related *CBF* genes were also inhibited by the deleted region since their expression was greater in the deletion mutant. This finding corroborates previous observations showing the coordinated control of the generative transition and freezing tolerance (Dhillon et al., 2010; Diallo et al., 2014; Galiba et al., 2009). The proteins encoded by the region deleted in the *mvp2* mutant proved to be positive regulators of several transcription factors (WRKY,

C2H2 Zn-finger) and heat shock proteins (HSP17, HSP80, HSP101) as indicated by the low expression of the corresponding genes in the mutants. The observed effect on HSPs gives a further evidence for the coordinated regulation of stress response and flowering. Gene ontology analysis based on biological processes indicated the effect of *mvp2* mutation on amino acid metabolism-related genes, while analysis of molecular functions showed the control of oxidoreductases and monooxygenases by the deleted chromosome region. The effect of whole chromosome 5A on amino acid metabolism at transcript and metabolite levels was shown in previous studies (Juhász et al., 2015; Kocsy et al., 2010; Kovács et al., 2011) and the present investigations demonstrated that the region with the *VRN1* gene is responsible for this effect. The results also indicate the involvement of redox processes in the control of the vegetative/generative transition (Diallo et al., 2014; Gulyás et al., 2014). A comparison of the genotypes related to the KEGG metabolic pathways indicated the effect of the mutation on flavonoid and steroid biosynthesis. These results are in good agreement with previous ones describing the role of flavonoids in the reproductive processes (Falcone Ferreyra et al., 2012). The various analyses of the transcriptome data also revealed the influence of *mvp2* mutation on the genes involved in the SA and cytokinin metabolism that is discussed in the next sections.

A large set of genes (198) was affected by the vegetative/generative transition independently of the *mvp2* mutation. These genes are not regulated by those ones located in the deleted region in *mvp2* mutant. Among others, the genes encoding a MYB transcription factor, a peroxidase and a protein kinase were upregulated and those encoding an RNA polymerase, a pre mRNA processing factor and an S-like RNase were down-regulated. This observation indicates the induction of regulatory genes and inhibition of the genes involved in the RNA metabolism during the vegetative/generative transition. Based on gene ontology analyses and alignment to KEGG metabolic pathways, the expression of genes related to carbohydrate metabolism, response to heavy metals, transition metal binding and carbon fixation was affected by the vegetative/generative transition. These results show that the energy homeostasis is modified during the generative transition.

8.2 Involvement of SA and cytokinins in the control of generative transition

The differences between wt and *mvp2* plants in the amount of SA and its precursors indicate the effect of the *VRN1* region on SA metabolism during the vegetative/generative transition in *T. monococcum*. Low temperature treatment induced certain components of SA biosynthetic routes including *o*HCA, BA and SA in the crowns and/or in the leaves. Earlier findings also showed that low temperature hardening of bread wheat (*T. aestivum*) in the light, but not in

the dark, led to a substantial increase in the bound *o*HCA level (Janda et al., 2007). Since these compounds may also serve as antioxidant compounds (Foley et al., 1999), their role in the maintaining of the redox balance was assumed. In the present work this increase was significant in both wt and *mvp2* plants and was detectable in the bound forms of these components indicating that the levels of free SA and, most probably, of the other related compounds are strictly controlled (Janda et al., 2014). These results indicated that SA significantly affects the initiation of flowering of wheat plants. Substantially lower total *o*HCA and SA levels were detected in the crowns of non-flowering *mvp2* mutant than in the wild-type plants at DR stage. This indicates that although SA is probably necessary for flowering initiation in wheat plants, its later existence is not required anymore. Similar findings were recently published in *Arabidopsis* plants, where transfer of plants from short- to long-day growth conditions was paralleled with a temporary increase in the SA level at pre-reproductive stages followed by a decline at the reproductive stage (Abreu and Munné-Bosch, 2009). In spite of the finding, that *Arabidopsis thaliana* plants impaired in SA accumulation or transport mechanisms flowered later than the wild-type (Martínez et al., 2004), which may indicate direct link between SA and floral development; exogenous treatment of *NahG Arabidopsis* plants with SA was not able to restore the wt flowering time (Martínez et al., 2004). However, it must be also mentioned that exogenous SA may be easily converted to bound form; therefore, the exact level of active SA cannot always be estimated (Szalai et al., 2011). The increase of biomass production during the reproductive stage and the final seed production in *NahG* transgenic and *sid2* mutant *Arabidopsis* plants (both with impaired SA accumulation capacity) in comparison to wild-type plants (Abreu and Munné-Bosch, 2009) may suggest SA function in cold acclimation and elevation of plant stress tolerance (associated with increased levels of protective compounds), which positively affects further development.

In cereals, the involvement of cytokinins has been studied during cold hardening (Kosová et al., 2012). Both cold tolerance and tillering ability were greatly increased in transgenic turf grass plants overproducing the cytokinin biosynthetic gene for isopentenyl transferase (Hu et al., 2005). However, less is known about their role in the development of generative phase in crops. The developmental changes are usually paralleled with altered hormonal levels. The elevation of cytokinins (and auxins) is associated with stimulation of meristematic activities in plants. Cytokinins control both check-points during cell cycle progression (Schaller et al., 2014). Isopentenyladenine of leaf origin was reported to trigger the floral transition in the shoot apical meristem of *Arabidopsis* (Bernier, 2013). Increased cytokinin concentration was

detected at the onset of vegetative-generative transition in *Brassica napus* (Tarkowská et al., 2012). Comparison of cytokinin profiles in *T. monococcum* spring line DV92 and winter line G3116 showed that the maximum of active cytokinins occurs at the onset of the early stage of reproductive development (Vanková et al., 2014). Spring line exhibited cytokinin maximum after 21 days, while winter line after 42 days when it fulfilled its vernalization requirement as indicated by the decrease of the frost tolerance and dehydrin levels. These data are in accordance with our results, which showed maximum of active cytokinins in DR stage. In wt, developmental transition was accompanied by subsequent fast down-regulation of cytokinins. During SI stage, when cell elongation and differentiation take place, other hormones, probably auxins and gibberellins, may exhibit their maxima.

Cytokinin elevation was also observed in *mvp2* mutant. Accumulation of predominantly *trans*-zeatin riboside and isopentenyladenosine may indicate tendency to overcome the developmental block in the mutant. Up-regulation of these compounds may indicate cytokinin transport from the roots. It might be also related to the cold acclimation of this genotype. Gradual cytokinin decrease during prolonged cold treatment (final sampling point) might reflect transition from acclimation to maintenance response phase (Larcher, 2003). Similarity of the response of cytokinin phosphates in both genotypes might be given by the prevailing effect of low temperature that negatively affects cytokinin biosynthesis and, as a consequence, plant growth rate.

The concentration of active cytokinins is controlled at transcriptional level by several multigene families including isopentenyl transferases for synthesis, cytokinin oxidases/dehydrogenases for degradation, *trans/cis*-zeatin O-glycosyltransferases for reversible inactivation and beta-glucosidases for reactivation (Song et al., 2012). Among them, a gene encoding zeatin O-glycosyltransferase was affected by the *mvp2* mutation and corresponding differences were found in *cis/trans*-zeatin O-glucoside content between wt and *mvp2* plants. Although we did not find such differences in the expression of other genes related to zeatin metabolism by transcript profiling, a coordinated regulation of these genes was observed during the reproductive development of maize in a previous study. It is possible to assume that differences in cytokinin related transcripts have not been detected in our study due to their relatively fine regulations, their subtle changes being below our threshold limit.

9 Conclusions

Comparison of wild type and *mvp2* deletion mutant wheat plants showed that the deleted region regulates a whole set of genes affecting freezing tolerance and vegetative/generative

transition. Among these genes also occur those ones that are related to SA and cytokinin metabolism, and may be responsible for the differences in the level of these hormones between the wild type and mutant plants. Thus, the present results indicate the involvement of these plant hormones in the VRN1-dependent control of flowering. Our results also contribute to the better understanding of the link between the stress responses and developmental processes in wheat plants.

10 Acknowledgements

The authors wish to thank Apollónia Horváthné and Mónika E. Fehér for their valuable help in plant cultivation and treatment. In addition, they would like to thank Krisztián Gierczik for his contribution to the real time experiments. This work was supported by the Hungarian Scientific Research Fund [OTKA CNK80781] and by the Ministry of Education, Youth and Sport of the Czech Republic through the National Program for Sustainability [LO1204].

11 References

Abreu, M.E., Munné-Bosch, S., 2009. Salicylic acid deficiency in *NahG* transgenic lines and *sid2* mutants increases seed yield in the annual plant *Arabidopsis thaliana*. J. Exp. Bot. 60, 1261–1271. doi:10.1093/jxb/ern363

Bernier, G., 2013. My favourite flowering image: the role of cytokinin as a flowering signal. J. Exp. Bot. 64, 5795–5799. doi:10.1093/jxb/err114

Breitkreutz, B.-J., Stark, C., Tyers, M., 2003. Osprey: a network visualization system. Genome Biol. 4, R22. doi:10.1186/gb-2003-4-3-r22

Chen, A., Li, C., Hu, W., Lau, M.Y., Lin, H., Rockwell, N.C., Martin, S.S., Jernstedt, J. a., Lagarias, J.C., Dubcovsky, J., 2014. PHYTOCHROME C plays a major role in the acceleration of wheat flowering under long-day photoperiod. Proc. Natl. Acad. Sci. 111, 10037–10044. doi:10.1073/pnas.1409795111

Dhillon, T., Pearce, S.P., Stockinger, E.J., Distelfeld, A., Li, C., Knox, A.K., Vashegyi, I., Vágújfalvi, A., Galiba, G., Dubcovsky, J., 2010. Regulation of freezing tolerance and flowering in temperate cereals: the VRN-1 connection. Plant Physiol. 153, 1846–1858. doi:10.1104/pp.110.159079

Diallo, A.O., Agharbaoui, Z., Badawi, M.A., Ali-Benali, M.A., Moheb, A., Houde, M., Sarhan, F., 2014. Transcriptome analysis of an mvp mutant reveals important changes in global gene expression and a role for methyl jasmonate in vernalization and flowering in wheat. J. Exp. Bot. 65, 2271–86. doi:10.1093/jxb/eru102

Distelfeld, A., Dubcovsky, J., 2010. Characterization of the *maintained vegetative phase* deletions from diploid wheat and their effect on *VRN2* and *FT* transcript levels. Mol. Genet. Genomics 283, 223–232. doi:10.1007/s00438-009-0510-2

Distelfeld, A., Li, C., Dubcovsky, J., 2009. Regulation of flowering in temperate cereals. Curr. Opin. Plant Biol. 12, 178–184. doi:10.1016/j.pbi.2008.12.010

Falcone Ferreyra, M.L., Rius, S.P., Casati, P., 2012. Flavonoids: biosynthesis, biological functions, and biotechnological applications. Front. Plant Sci. 3, 1–15. doi:10.3389/fpls.2012.00222

Foley, S., Navaratnam, S., McGarvey, D.J., Land, E.J., Truscott, T.G., Rice-Evans, C.A., 1999. Singlet oxygen quenching and the redox properties of hydroxycinnamic acids. Free Radic. Biol. Med. 26, 1202–1208. doi:10.1016/S0891-5849(98)00313-X

Galiba, G., Vágújfalvi, A., Li, C., Soltész, A., Dubcovsky, J., 2009. Regulatory genes involved in the determination of frost tolerance in temperate cereals. Plant Sci. 176, 12–19. doi:10.1016/j.plantsci.2008.09.016

Gardner, J.S., Hess, W.M., Trione, E.J., 2007. Development of the Young Wheat Spike: A Sem Study of Chinese Spring Wheat.

Gulick, P.J., Drouin, S., Yu, Z., Danyluk, J., Poisson, G., Monroy, A.F., Sarhan, F., 2005. Transcriptome comparison of winter and spring wheat responding to low temperature. Genome 48, 913–923. doi:10.1139/g05-039

Gulyás, Z., Boldizsár, A., Novák, A., Szalai, G., Pál, M., Galiba, G., Kocsy, G., 2014. Central role of the flowering repressor ZCCT2 in the redox control of freezing tolerance and the initial development of flower primordia in wheat. BMC Plant Biol. 14, 91. doi:10.1186/1471-2229-14-91

Hu, Y., Jia, W., Wang, J., Zhang, Y., Yang, L., Lin, Z., 2005. Transgenic tall fescue containing the *Agrobacterium tumefaciens ipt* gene shows enhanced cold tolerance. Plant Cell Rep. 23, 705–709. doi:10.1007/s00299-004-0863-2

Janda, T., Gondor, O.K., Yordanova, R., Szalai, G., Pál, M., 2014. Salicylic acid and photosynthesis: signalling and effects. Acta Physiol. Plant. 36, 2537–2546. doi:10.1007/s11738-014-1620-y

Janda, T., Szalai, G., Leskó, K., Yordanova, R., Apostol, S., Popova, L.P., 2007. Factors contributing to enhanced freezing tolerance in wheat during frost hardening in the light. Phytochemistry 68, 1674–1682. doi:10.1016/j.phytochem.2007.04.012

Juhász, Z., Boldizsár, Á., Nagy, T., Kocsy, G., Marincs, F., Galiba, G., Bánfalvi, Z., 2015. Pleiotropic effect of chromosome 5A and the mvp mutation on the metabolite profile during cold acclimation and the vegetative/generative transition in wheat. BMC Plant Biol. 15, 57. doi:10.1186/s12870-014-0363-7

Kasukabe, Y., He, L.X., Nada, K., Misawa, S., Ihara, I., Tachibana, S., 2004. Overexpression of spermidine synthase enhances tolerance to multiple environmental stresses and up-regulates the expression of various stress regulated genes in transgenic Arabidopsis thaliana. Plant Cell Physiol. 45, 712–722. doi:10.1093/pcp/pch083

Kocsy, G., Athmer, B., Perovic, D., Himmelbach, A., Szucs, A., Vashegyi, I., Schweizer, P., Galiba, G., Stein, N., 2010. Regulation of gene expression by chromosome 5A during cold hardening in wheat. Mol. Genet. Genomics 283, 351–63. doi:10.1007/s00438-010-0520-0

Kosová, K., Prášil, I.T., Vítámvás, P., Dobrev, P., Motyka, V., Floková, K.K., Novák, O., Turečková, V., Rolčik, J., Pešek, B., Trávničková, A., Gaudinová, A., Galiba, G., Janda, T., Vlasáková, E., Prášilová, P., Vanková, R., 2012. Complex phytohormone responses during the cold acclimation of two wheat cultivars differing in cold tolerance, winter Samanta and spring Sandra. J. Plant Physiol. 169, 567–576. doi:10.1016/j.jplph.2011.12.013

Kovács, Z., Simon-Sarkadi, L., Sovány, C., Kirsch, K., Galiba, G., Kocsy, G., 2011. Differential effects of cold acclimation and abscisic acid on free amino acid composition in wheat. Plant Sci. 180, 61–68. doi:10.1016/j.plantsci.2010.08.010

Krizek, B.A., 2011. Auxin regulation of Arabidopsis flower development involves members of the AINTEGUMENTA-LIKE/PLETHORA (AIL/PLT) family. J. Exp. Bot. 62, 3311–3319. doi:10.1093/jxb/err127

Krochko, J.E., Abrams, G.D., Loewen, M.K., Abrams, S.R., Cutler, A.J., 1998. (+)-Abscisic Acid 8 -Hydroxylase Is a Cytochrome P450 Monooxygenase. Plant Physiol. 118, 849–860. doi:10.1104/pp.118.3.849

Larcher, W., 2003. Physiological plant ecology: ecophysiology and stress physiology of functional groups, 4th ed. Springer-Verlag, Berlin, Heidelberg.

Laurie, D.A., 1997. Comparative genetics of flowering time. Plant Mol. Biol. 35, 167–177. doi:10.1023/A:1005726329248

Lee, H., Suh, S.S., Park, E., Cho, E., Ahn, J.H., Kim, S.G., Lee, J.S., Kwon, Y.M., Lee, I., 2000. The AGAMOUS-LIKE 20 MADS domain protein integrates floral inductive pathways in *Arabidopsis*. Genes Dev. 14, 2366–2376. doi:10.1101/gad.813600

Lomin, S.N., Krivosheev, D.M., Steklov, M.Y., Arkhipov, D. V., Osolodkin, D.I.,

Schmülling, T., Romanov, G.A., 2015. Plant membrane assays with cytokinin receptors underpin the unique role of free cytokinin bases as biologically active ligands. J. Exp. Bot. 66, 1851–1863. doi:10.1093/jxb/eru522

Loukoianov, A., Yan, L., Blechl, A., Sanchez, A., Dubcovsky, J., 2005. Regulation of VRN-1 vernalization genes in normal and transgenic polyploid wheat. Plant Physiol. 138, 2364–2373. doi:10.1104/pp.105.064287

Maere, S., Heymans, K., Kuiper, M., 2005. BiNGO: a Cytoscape plugin to assess overrepresentation of Gene Ontology categories in Biological Networks. Bioinformatics 21, 3448–3449. doi:10.1093/bioinformatics/bti551

Majláth, I., Szalai, G., Soós, V., Sebestyén, E., Balázs, E., Vanková, R., Dobrev, P.I., Tari, I., Tandori, J., Janda, T., 2012. Effect of light on the gene expression and hormonal status of winter and spring wheat plants during cold hardening. Physiol. Plant. 145, 296–314. doi:10.1111/j.1399-3054.2012.01579.x

Martínez, C., Pons, E., Prats, G., León, J., 2004. Salicylic acid regulates flowering time and links defence responses and reproductive development. Plant J. 37, 209–217. doi:10.1046/j.1365-313X.2003.01954.x

Meuwly, P., Métraux, J.P., 1993. Ortho-anisic acid as internal standard for the simultaneous quantitation of salicylic acid and its putative biosynthetic precursors in cucumber leaves. Anal. Biochem. doi:10.1006/abio.1993.1529

Monroy, A.F., Dryanova, A., Malette, B., Oren, D.H., Ridha Farajalla, M., Liu, W., Danyluk, J., Ubayasena, L.W.C., Kane, K., Scoles, G.J., Sarhan, F., Gulick, P.J., 2007. Regulatory gene candidates and gene expression analysis of cold acclimation in winter and spring wheat. Plant Mol. Biol. 64, 409–423. doi:10.1007/s11103-007-9161-z

Mutasa-Gottgens, E., Hedden, P., 2009. Gibberellin as a factor in floral regulatory networks. J. Exp. Bot. 60, 1979–1989. doi:10.1093/jxb/erp040

Onouchi, H., Igeno, M.I., Perilleux, C., Graves, K., Coupland, G., 2000. Mutagenesis of plants overexpressing *CONSTANS* demonstrates novel interactions among Arabidopsis flowering-time genes. Plant Cell 12, 885–900. doi:10.1105/tpc.12.6.885

Oughtred, R., Chatr-aryamontri, A., Breitkreutz, B.-J., Chang, C.S., Rust, J.M., Theesfeld, C.L., Heinicke, S., Breitkreutz, A., Chen, D., Hirschman, J., Kolas, N., Livstone, M.S., Nixon, J., O'Donnell, L., Ramage, L., Winter, A., Reguly, T., Sellam, A., Stark, C., Boucher, L., Dolinski, K., Tyers, M., 2016. BioGRID: A Resource for Studying Biological Interactions in Yeast. Cold Spring Harb. Protoc. doi:10.1101/pdb.top080754

Pál, M., Horváth, E., Janda, T., Páldi, E., Szalai, G., 2005. Cadmium stimulates the accumulation of salicylic acid and its putative precursors in maize (Zea mays) plants. Physiol. Plant. 125, 356–364. doi:10.1111/j.1399-3054.2005.00545.x

Paolacci, A.R., Tanzarella, O.A., Porceddu, E., Ciaffi, M., 2009. Identification and validation of reference genes for quantitative RT-PCR normalization in wheat. BMC Mol. Biol. 10, 11. doi:10.1186/1471-2199-10-11

Schaller, G.E., Street, I.H., Kieber, J.J., 2014. Cytokinin and the cell cycle. Curr. Opin. Plant Biol. 21, 7–15. doi:10.1016/j.pbi.2014.05.015

Shitsukawa, N., Ikari, C., Mitsuya, T., Sakiyama, T., Ishikawa, A., Takumi, S., Murai, K., 2007a. Wheat *SOC1* functions independently of *WAP1/VRN1*, an integrator of vernalization and photoperiod flowering promotion pathways. Physiol. Plant. 130, 627–

636. doi:10.1111/j.1399-3054.2007.00927.x

Shitsukawa, N., Ikari, C., Shimada, S., Kitagawa, S., Sakamoto, K., Saito, H., Ryuto, H., Fukunishi, N., Abe, T., Takumi, S., Nasuda, S., Murai, K., 2007b. The einkorn wheat (Triticum monococcum) mutant, maintained vegetative phase, is caused by a deletion in the VRN1 gene. Genes Genet. Syst. 82, 167–170. doi:10.1266/ggs.82.167

Song, J., Jiang, L., Jameson, P., 2012. Co-ordinate regulation of cytokinin gene family members during flag leaf and reproductive development in wheat. BMC Plant Biol. 12, 78. doi:10.1186/1471-2229-12-78

Svačinova, J., Novák, O., Plačková, L., Lenobel, R., Holík, J., Strnad, M., Doležal, K., 2012. A new approach for cytokinin isolation from Arabidopsis tissues using miniaturized purification: pipette tip solid-phase extraction. Plant Methods 8, 17. doi:10.1186/1746-4811-8-17

Szalai, G., Horgosi, S., Soós, V., Majláth, I., Balázs, E., Janda, T., 2011. Salicylic acid treatment of pea seeds induces its *de novo* synthesis. J. Plant Physiol. 168, 213–219. doi:10.1016/j.jplph.2010.07.029

Tarkowská, D., Filek, M., Biesaga-Kościelniak, J., Marcińska, I., Macháčková, I., Krekule, J., Strnad, M., 2012. Cytokinins in shoot apices of *Brassica napus* plants during vernalization. Plant Sci. 187, 105–112. doi:10.1016/j.plantsci.2012.02.003

Vanková, R., Kosová, K., Dobrev, P., Vítámvás, P., Trávníčková, A., Cvikrová, M., Pešek, B., Gaudinová, A., Prerostová, S., Musilová, J., Galiba, G., Prášil, I.T., 2014. Dynamics of cold acclimation and complex phytohormone responses in Triticum monococcum lines G3116 and DV92 differing in vernalization and frost tolerance level. Environ. Exp. Bot. 101, 12–25. doi:10.1016/j.envexpbot.2014.01.002

Winfield, M.O., Lu, C., Wilson, I.D., Coghill, J.A., Edwards, K.J., 2009. Cold- and light-induced changes in the transcriptome of wheat leading to phase transition from vegetative to reproductive growth. BMC Plant Biol. 9, 55. doi:10.1186/1471-2229-9-55

Worland, A.J., 1996. The influence of flowering time genes on environmental adaptability in European wheats. Euphytica 89, 49–57. doi:10.1007/BF00015718

Yan, L., Loukoianov, A., Tranquilli, G., Helguera, M., Fahima, T., Dubcovsky, J., 2003. Positional cloning of the wheat vernalization gene VRN1. Proc. Natl. Acad. Sci. U. S. A. 100, 6263–8. doi:10.1073/pnas.0937399100

Yu, H., Xu, Y., Tan, E.L., Kumar, P.P., 2002. AGAMOUS-LIKE 24, a dosage-dependent mediator of the flowering signals. PNAS 99, 16336–16341. doi:10.1073/pnas.212624599

12 Figure legends

Figure 1.: Morphology of the shoot apices during vegetative/generative transition. The following developmental stages are shown: vegetative phase before the start of cold treatment (growth at 20/17 °C) (VP 20 °C), vegetative phase at 4 °C (VP 4 °C), double ridge stage (DR) and initiation of spike primordia (SI). Only the apices of *Triticum monococcum* wt showed these phenophase changes. The morphology of *mvp2* mutant apices remained very similar during the treatment – aside from a short elongation – because this genotype cannot flower. The four sampling points were chosen according the wt development, but the same nomenclature was used in case of the mutant genotype. The white bars indicate 100 μm.

Figure 2.: Set diagram of the genes which exhibited higher than 2 fold-change of expression in relation to the genotype (G), developmental phase (D) or their interaction (D × G). (According to two way ANOVA.)

Figure 3.: Relative expression of the genes used for the validation of the microarray results. A - *CBF4* (C repeat-binding factor4); B - *CBF14* (C repeat-binding factor14); C - *R2R3-MYB* (R2R3-MYB protein); D - *VRN1* (vernalization 1); E - *C2H2* (C2H2 Zn finger protein); F - *STPK* (serine-threonine protein kinase); G - *LG* (lipoxygenase); H - *HSP80* (heat shock protein 80 KDa); I - *HSP101* (heat shock protein 101 KDa); J - *HSP17* (small heat shock protein 17.3 KDa); K - *MPBF1* (multiprotein bridging factor 1); L - *PAL* (phenylalanine ammonia-lyase). All the expression values were compared to those detected in wt at DR phase. $\Delta\Delta C_t$ method was used for the data analysis. All y-axes show the relative normalized expression at $\log_2$ scale. The error bars show the standard deviation.

Figure 4.: Filtered heat-map of the selected genes differentially expressed in *mvp2* and wt plants at the DR phase, which exhibited expression difference higher than 2 or smaller than 0.5.

Figure 5.: Networks of interacting proteins. The main coding genes (*AP1, SEP4, SAG12* and *PHYC*, i.e., the homologs of the genes deleted in the *mvp2* mutant: *VRN1*, *AGLG1, CYS* and *PHY-C,* respectively) are indicated by deep blue circles. Genes that were not represented in the array experiment are indicated by light blue and smaller circles. All other genes received a special three-parted specification. Left sector represents the relative expression of *mvp2* at DR phase compared to wt at DR. Right sector represents the expression of wt at SI phase compared to wt at DR. The bottom sector represents the expression of *mvp2* at SI phase compared to wt at DR. Direct connections are shown with red lines, while the indirect connections with orange and black lines.

Figure 6.: Salicylic acid biosynthesis and the changes in the crowns and leaves of the examined plants. Accumulation of bound and free 2-hydroxy-cinnamic acid (*o*HCA) in crowns (A) and leaves (B), of bound and free cinnamate (CA) in crowns (C) and leaves (D), of bound and free salicylic acid (SA) in crowns (E) and leaves (F) and of bound and free benzoate (BA) in crowns (G) and leaves (H).

Figure 7.: Comparison of cytokinin content in the leaves of *mvp2* mutant and wt during the vegetative/generative transition at 4 °C. A – cytokinin metabolites down-regulated in *mvp2* mutant; B - cytokinin metabolites up-regulated in *mvp2* mutant.

Supplemental Figure 1: Regression analysis between micro-array and qRT-PCR. Relative fold changes in *mvp2* at DR, *mvp2* at SI, wt at DR and wt at SI. In every case expression values were compared to wt at DR. ‘x’ coordinates show the result in micro-array, ‘y’ coordinates show the results in qRT-PCR.

Supplemental Figure 2: Expression pattern of genes that exhibit more than 2-fold difference (on $\log_2$ scale) in the expression rate of genotypes and/or developmental stages. In the first column, two developmental phases (DR and SI) of wt were compared to each other; in the second and third columns, SI and DR phases of *mvp2* was compared to the DR phase of wt. These 200 genes represent well-annotated, non-redundant wheat proteins with E-value ≤ 1e-40.

Supplemental Figure 3: Result of gene ontology analysis according to biological processes. The diagram shows the number of the genes associated with the specified process. In the right bottom of the figure the set-diagram represents the clusters of pathways in connection with the genotype (G), developmental phase (D) and both (D × G-D-G).

Supplemental Figure 4: Result of gene ontology analysis according to molecular functions. The diagram shows the number of the genes associated with the specified functions. In the right bottom of the figure the set-diagram represents the clusters of pathways in connection with the genotype (G), developmental phase (D) and both (D × G-D-G).

Supplemental Figure 5: Clusterisation of the genes in connection with KEGG pathways. In the right bottom of the figure the set-diagram represents the clusters of pathways.

Supplemental Figure 6: Zeatin biosynthesis according to the KEGG database. All of the measured cytokinins are marked with blue circles.

Supplemental Figure 7: Cytokinin content in the leaves of the examined plants during the vegetative/generative transition at 4 °C. Cytokinin metabolites were grouped according to molecular structure and biological activity. A – cytokinin bases ; B – cytokinin ribosides; C – cytokinin monophosphates; D – cytokinin N-glucosides; E – cytokinin O-glucosides.

Supplemental Table 1: Primers sequences.

Supplemental Table 2: Genes selected for the analyses.
Row A represents the selected genes whose expression changes were visualized on the heat-maps (Fig. 4 and Supp. Fig. 2). The full heat-map (Supp. Fig. 2) represents 200 genes (A/5). Only those were selected for the reduced map (Fig. 4) that exhibited differences between the genotypes at DR phase smaller than 0.5 or bigger than 2 (A/6).
Row B presents the dataset selection for gene ontology analysis. In B/2 cells numbers of those genes are indicated where the changes between the compared groups were higher than or equal to 2 [D: according to development phase (DR and SI); G: according to genotype (*mvp2* and wt) and D × G-D-G: according to common set of D, G and D × G] and the p-value ≤ 0.05. *Arabidopsis* homologs were selected based on this dataset if the E-value ≤ 1e-40 (B/3). Only those expression results related to the same genes were kept that exhibited the best E-values (B/4). The selected genes were analysed by BiNGO Cytoscape plugin software to determine over-represented genes connected to biological processes (B/5) and molecular functions (B/6). For the functional annotation of genes, KEGG database was used (B/7).
Row C shows the selected dataset of those genes that were visualized in Fig. 5 showing networks of interacting proteins. In the end, 59 genes (Arabidopsis homologs) were identified in the BioGrid network.

Figure1

Click here to download high resolution image

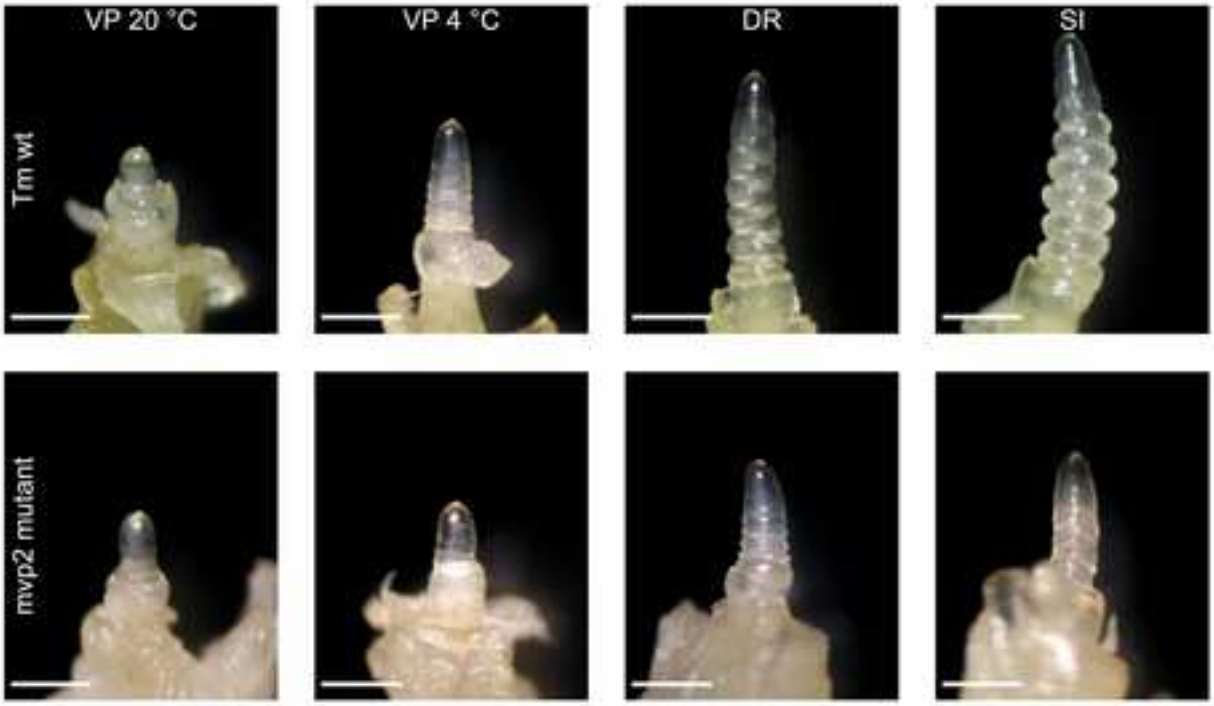

Figure2

Click here to download high resolution image

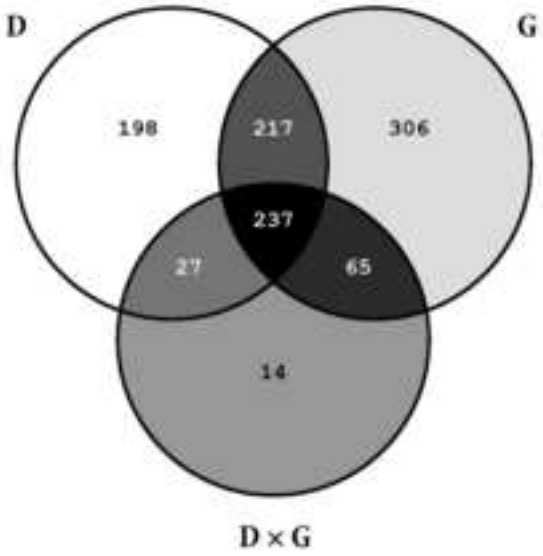

Figure3

Click here to download high resolution image

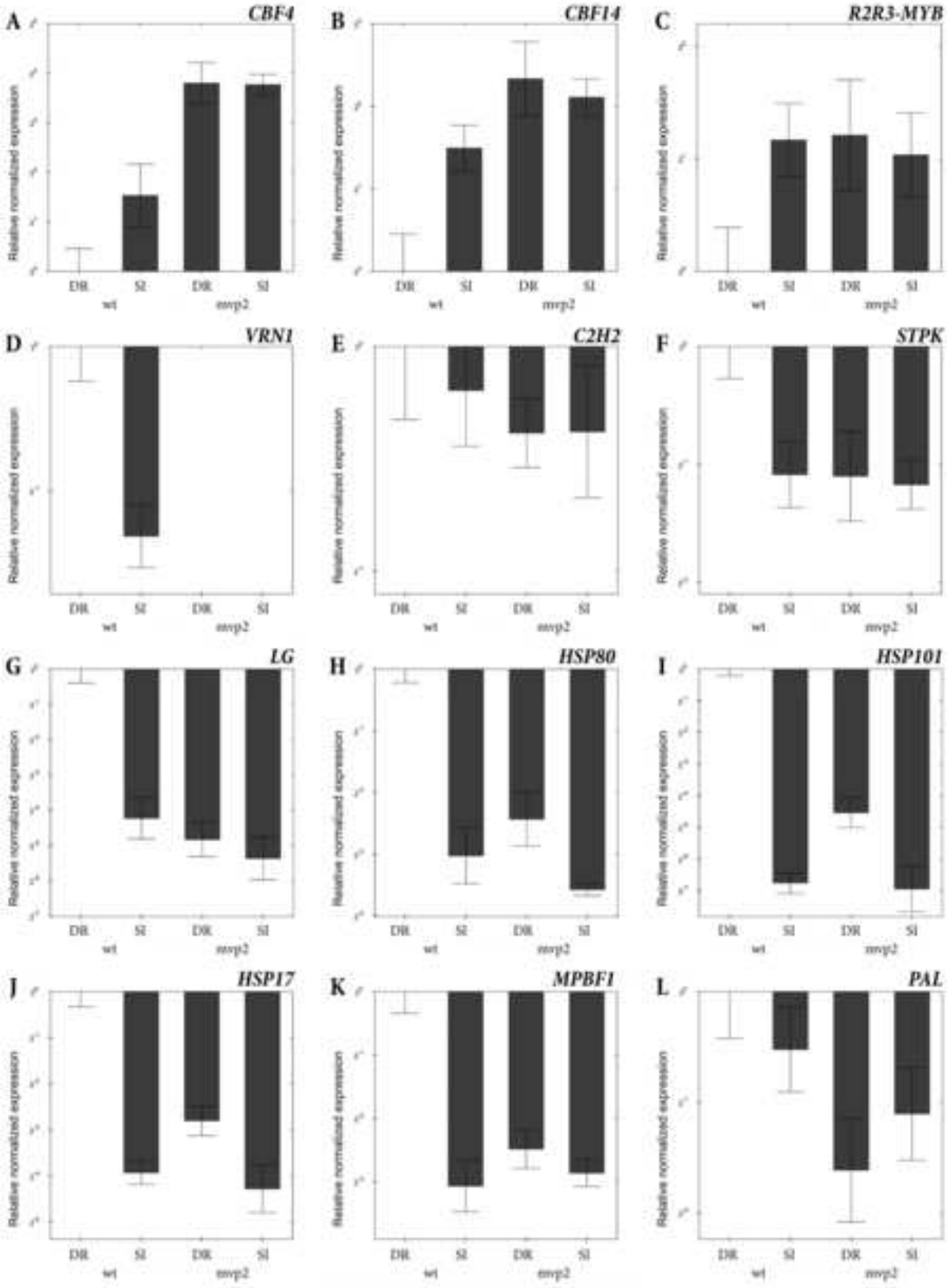

Figure4

Click here to download high resolution image

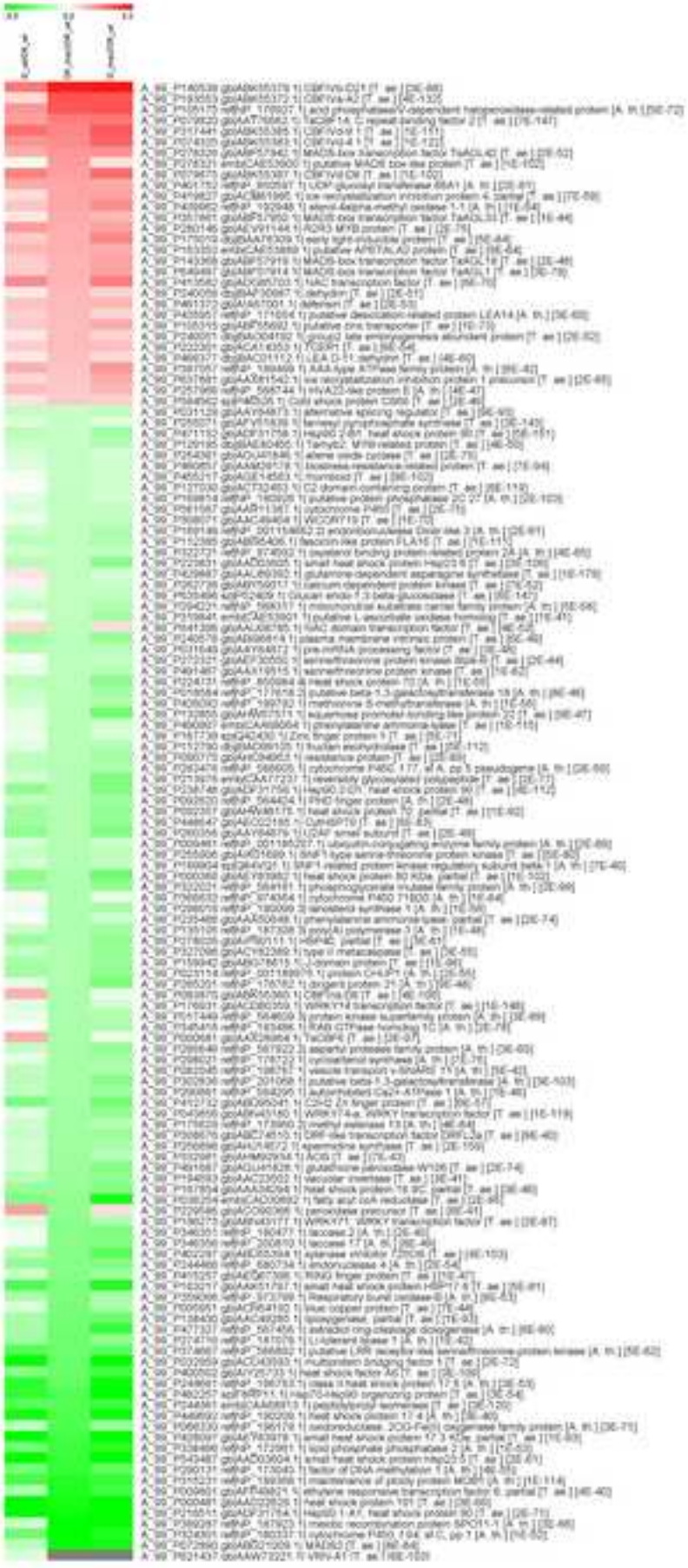

Figure5

Click here to download high resolution image

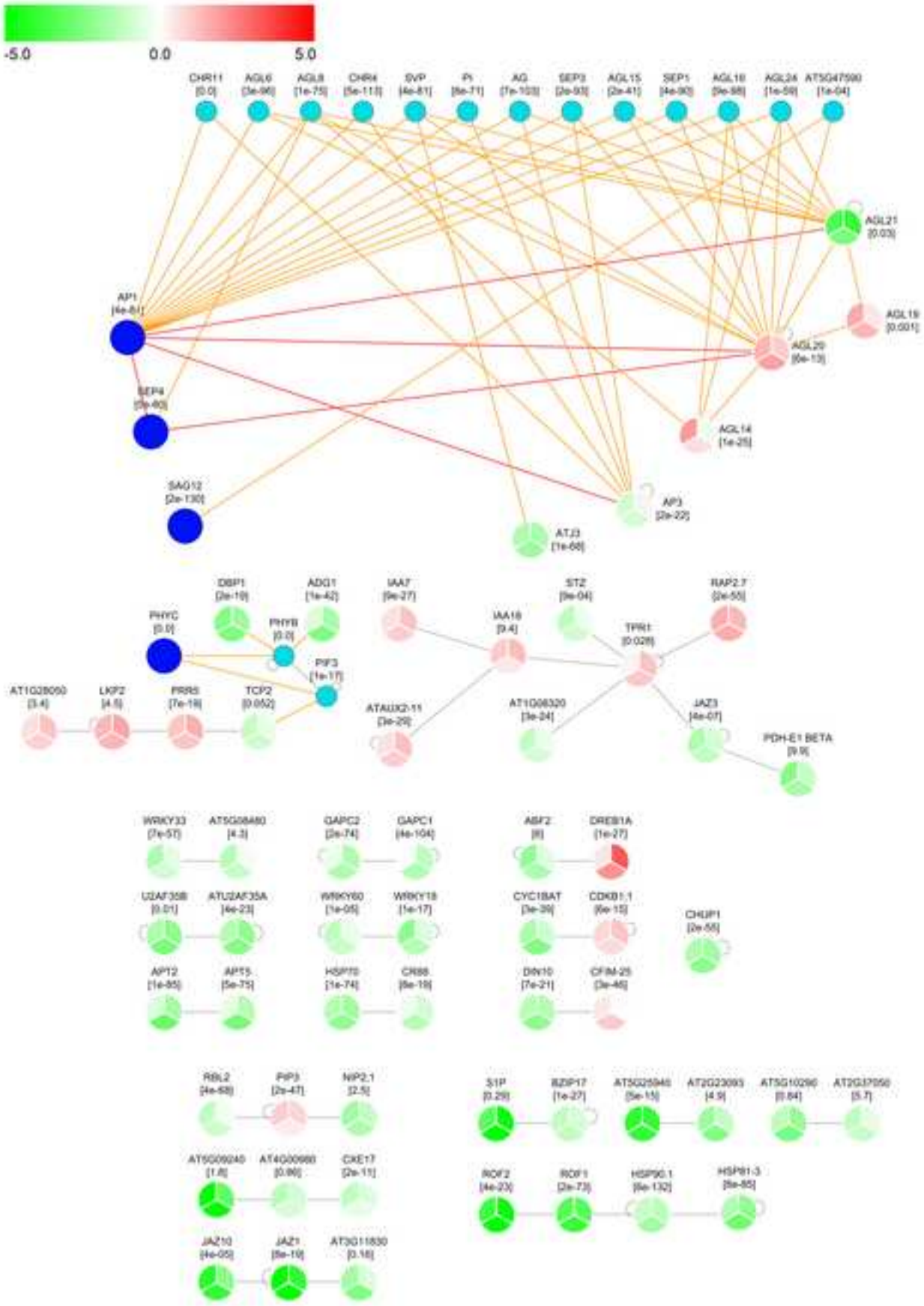

Figure6

Click here to download high resolution image

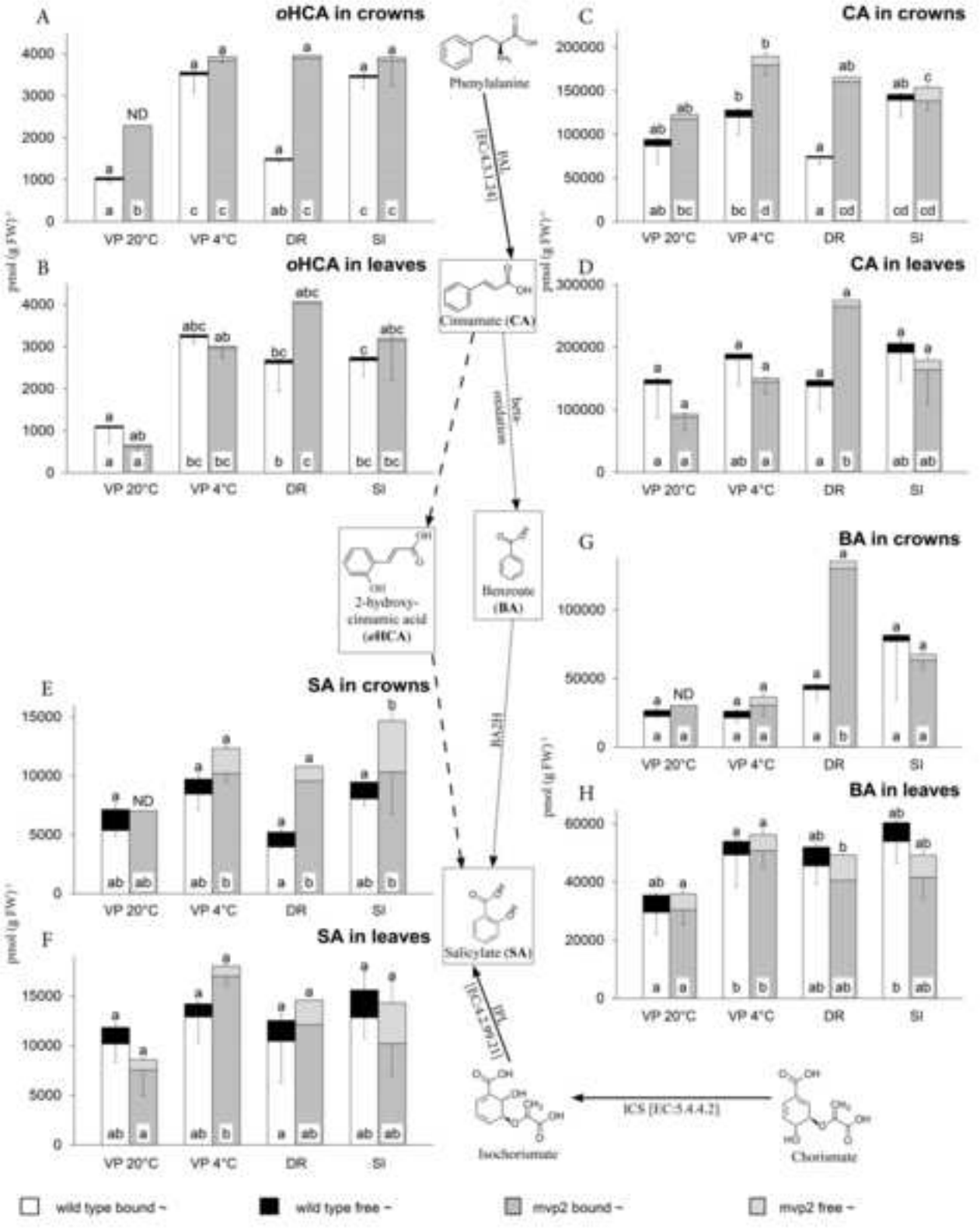

Figure7

Click here to download high resolution image

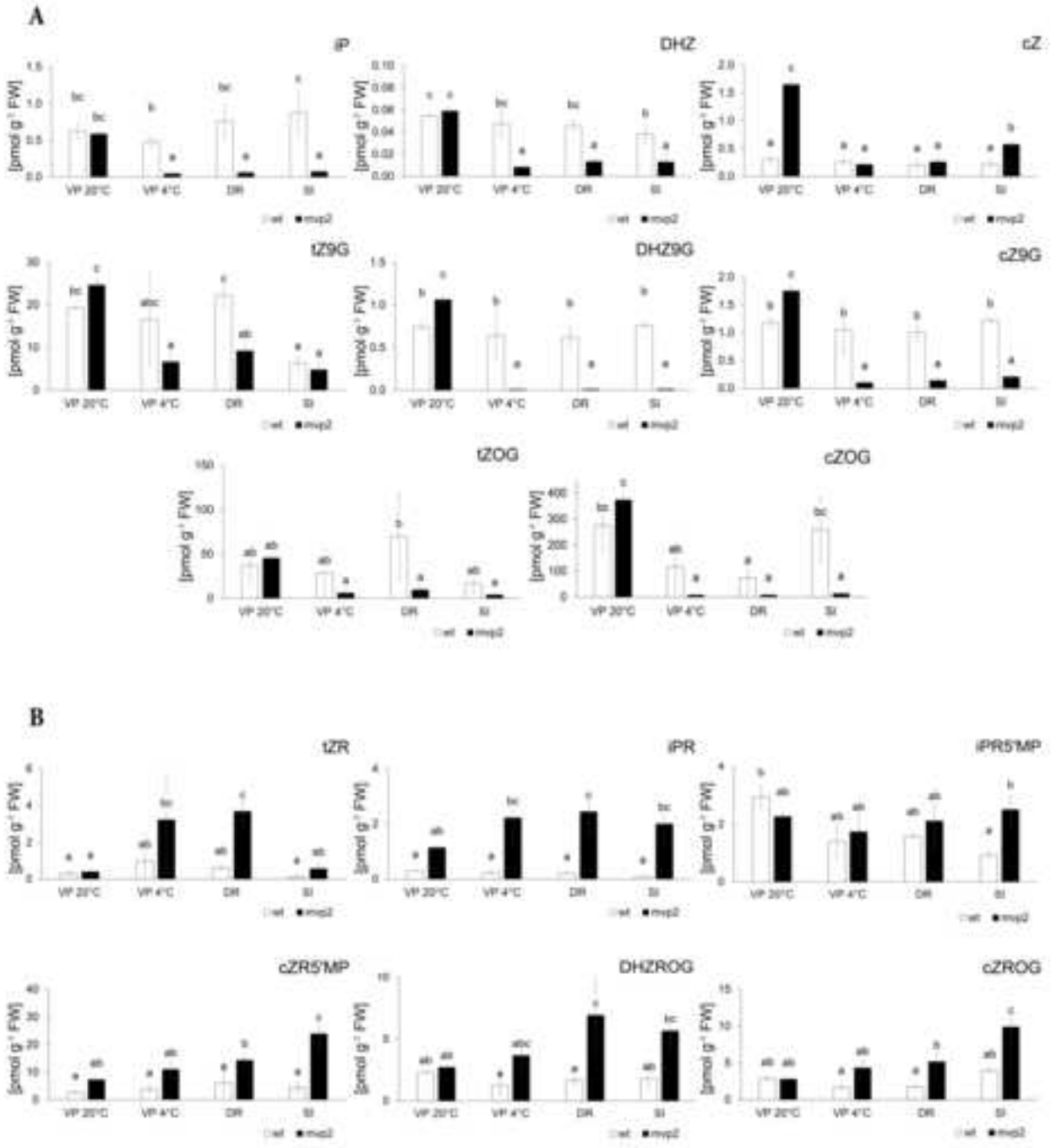

Suppl.Figure1

Click here to download high resolution image

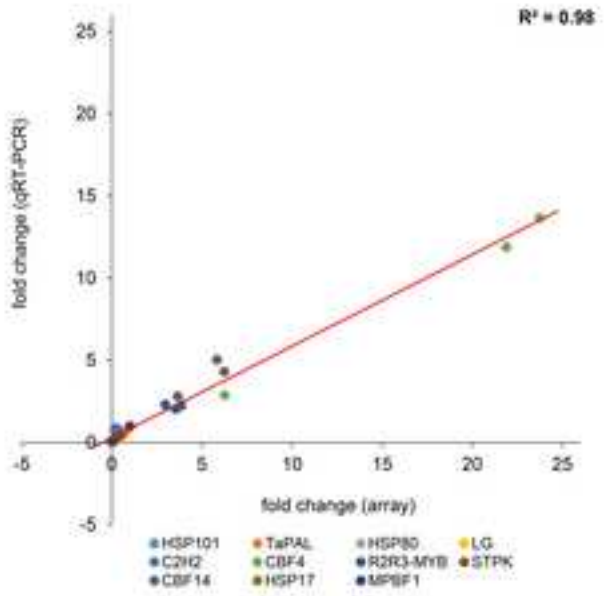

Suppl.Figure2

Click here to download Figure: S2 full heat map.pdf

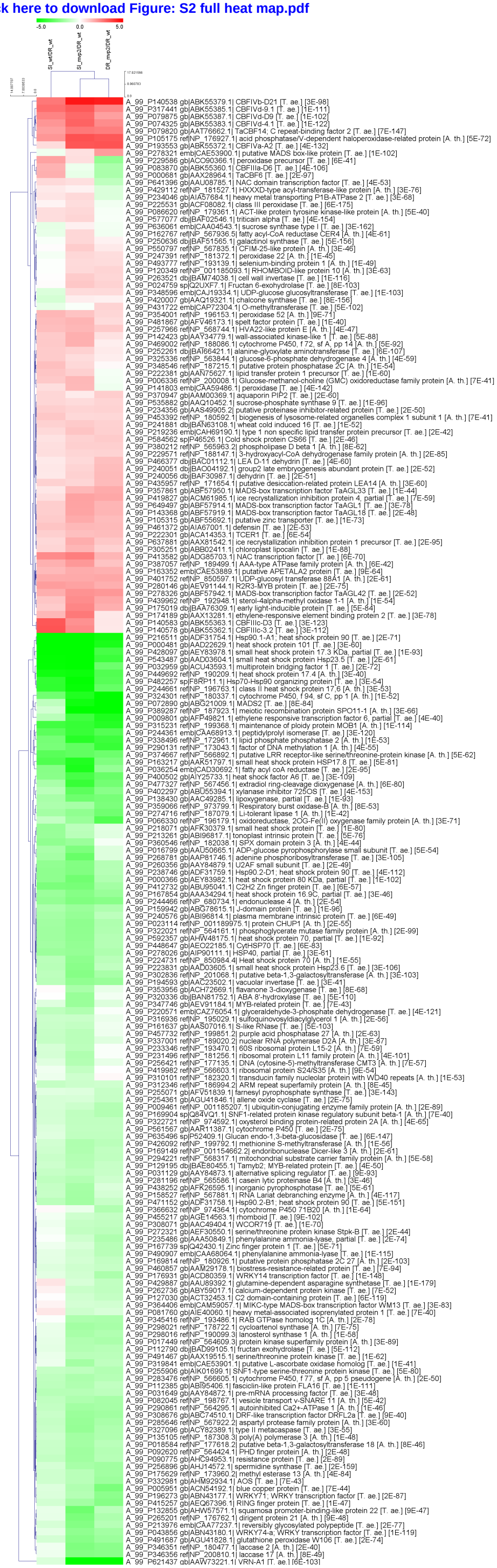

Suppl.Figure3

Click here to download high resolution image

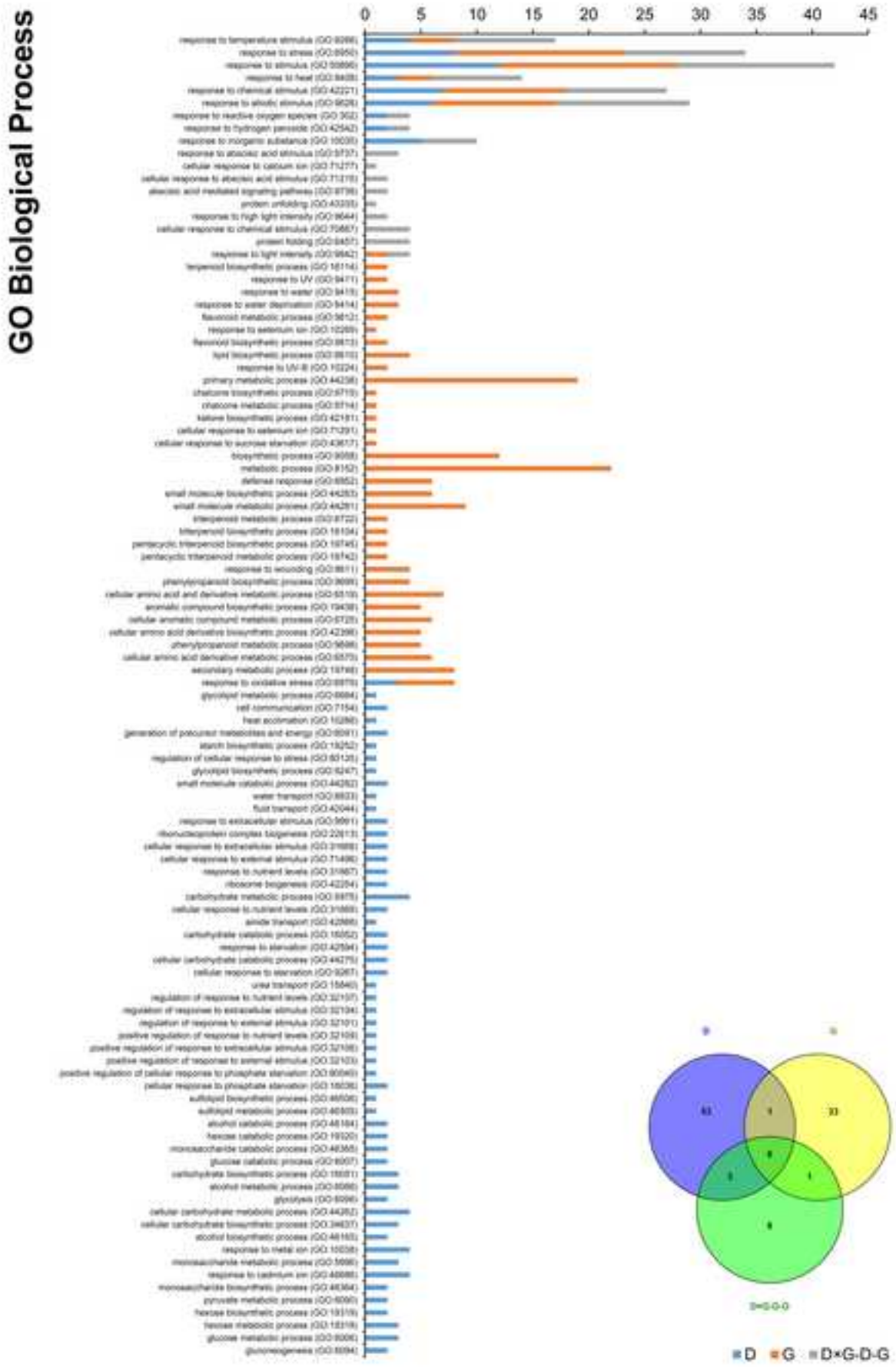

Suppl.Figure4

Click here to download high resolution image

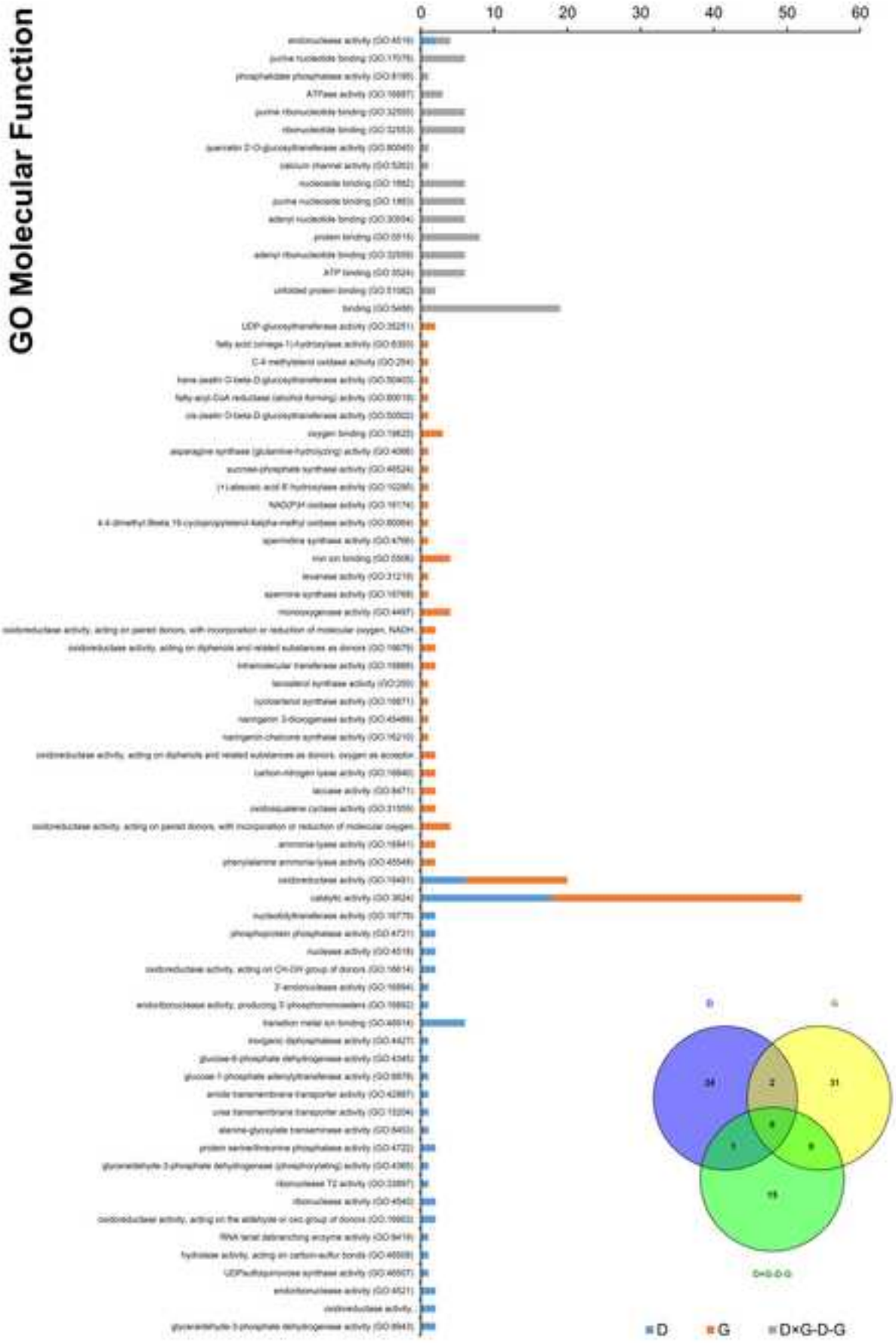

Suppl.Figure5

Click here to download high resolution image

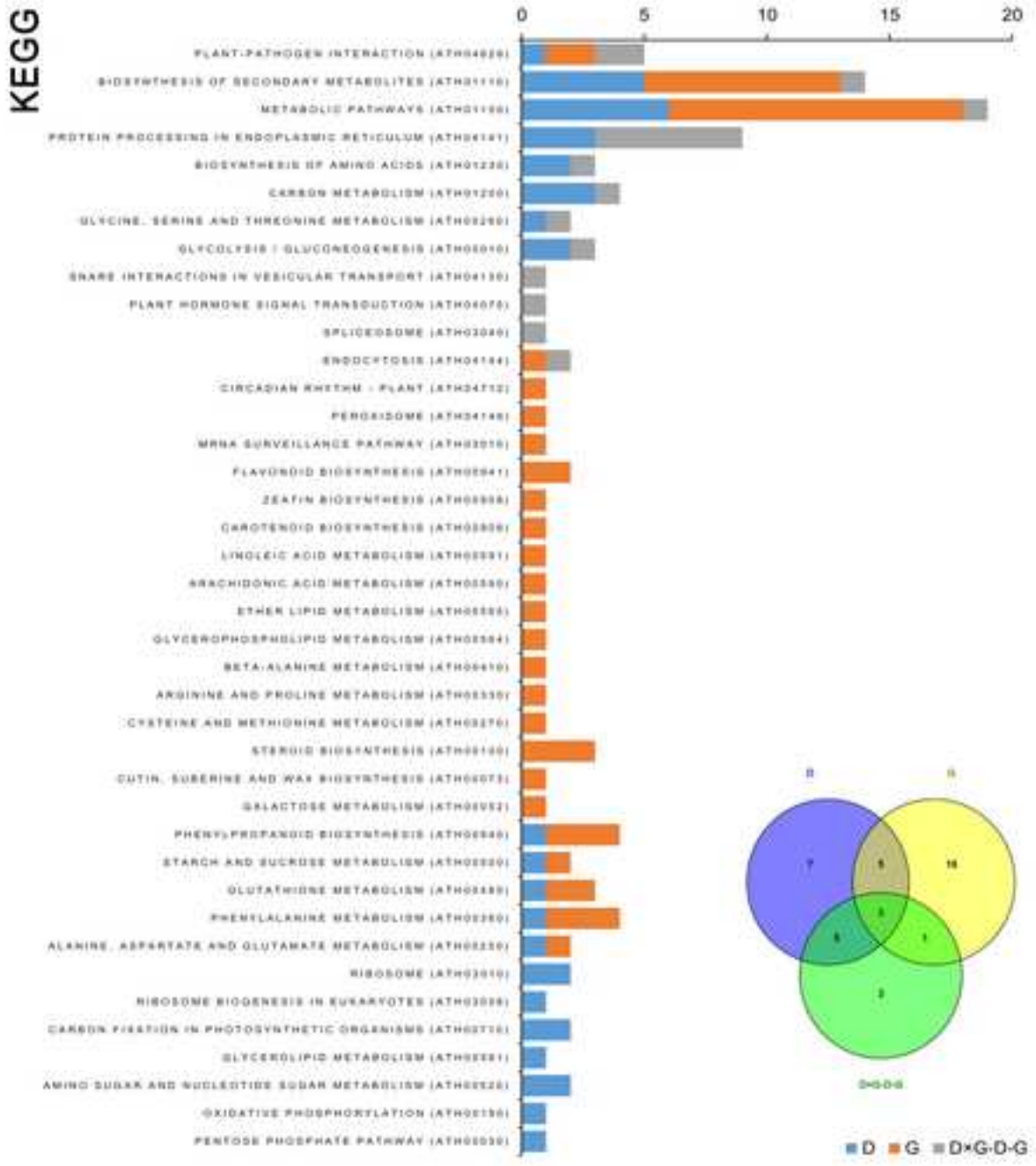

Suppl.Figure6

Click here to download high resolution image

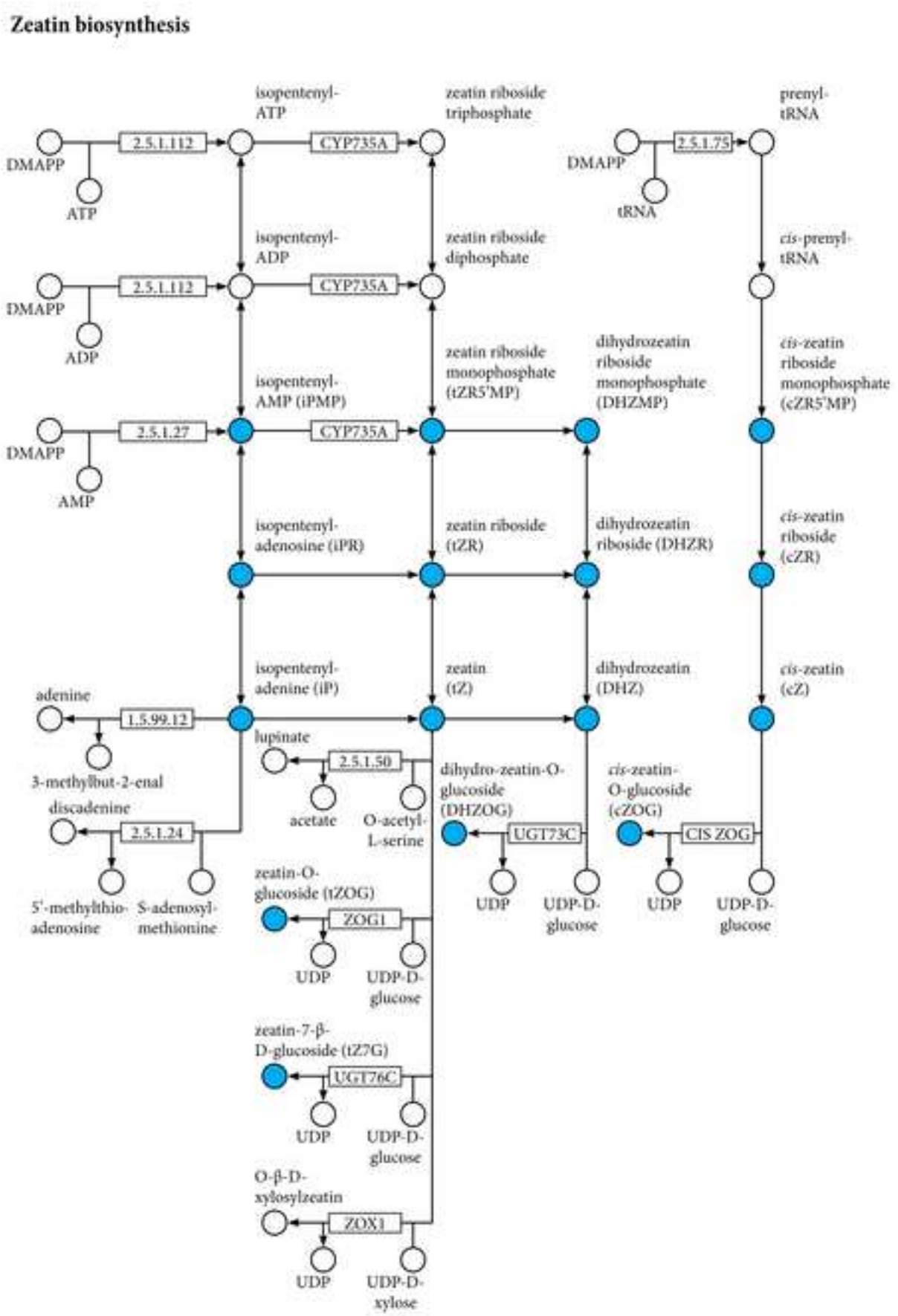

Suppl.Figure7

Click here to download high resolution image

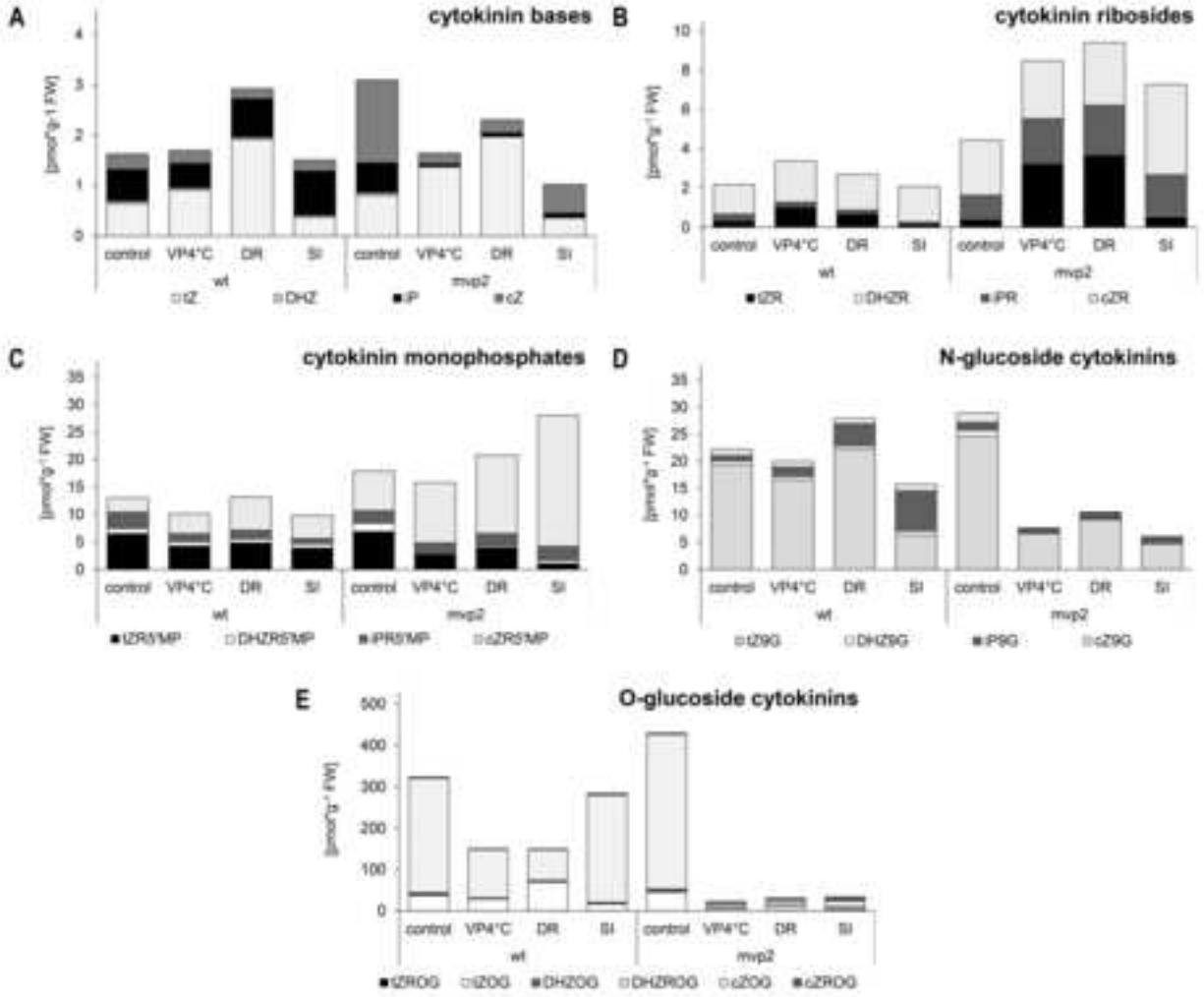

Suppl.Table1

Name	Function	Forward	Reverse	Amplicon length	Reference	GeneID
mvp-CBF4	C repeat-binding factor4	GGCGGGGAGGATCAAGTACAA	GAATCGGCGAAGTTGAGGCAG	222 bp		ABK55379.1
mvp-CBF14	C repeat-binding factor14	AAGGAGATCAAGGACGCCGTC	CCGAGTAGAACGATCCGGCAT	208 bp		AAT76662.1
mvp-STPK	serine-threonine protein kinase	CTCCGTTCGGTCCGTGAATCT	GCCCGAGCCTATGTCCTTGAT	157 bp		AIK01699.1
mvp-R2R3MYB	R2R3-MYB protein	TTGGTCGTCGATCCTCCACAG	GAGGAGAAGAAGGCGGAGGTG	210 bp		AEV91144.1
mvp-LG	lipoxygenase	TGGGCCAGCAAAATTCCCCTA	GCCACTCATGAAACGTGCACA	195 bp		AAC49285.1
mvp-C2H2	C2H2 Zn finger protein	TCGATGCAGATCCACCACGAG	TACCCCGTCTTCTTGAGGCTG	164 bp		ABU95041.1
mvp-HSP17	heat shock protein 17.3 KDa	CATCAAGGTGCAGGTGGAGGA	CCTGGATGGTCTTGGGCTTCT	242 bp		X58279.1
mvp-MPBF1	multiprotein bridging factor 1	GACGAACAAGAATGCCTCCGC	CTCTCGTACTCCTGCACCACC	201 bp		GQ370008.1
mvp-HSP80	heat shock protein 80 KDa	TTCCAGGCCGAGATCAACCAG	GTGTGTTCGTGGCCTTGTCAG	202 bp		AEY83982.1
mvp-HSP101	heat shock protein 101 KDa	GGTGACGCAGCTGTCCAAGAT	AGGATGTCGGACCTCTGCCC	153 bp		AAD22629.1
VRN-1	MADS-box transcription factor	ACAAGAAAAACACTTGCAGAGAAGTTCAGC	CATGGTAAATTACTCGTACAGCCATCTCAGC	1084 bp	(Juhász et al. 2015)	AY747599.1
mvp F18 and mvp R22		AGCCACAAGAACCGGGACTA	ATTCAAGCCCCAATGTTCTC	172 bp	(Dhillon et al. 2010)	AY747599.1
mvp F18 and mvp R23		AGCCACAAGAACCGGGACTA	CCCAAACTTTGCGGTGTATC	339 bp		AY747599.1
Ex4-5 and Ex8_R1-ABD		TCAGATCCAGGAAGAACCAA	TTGATGTGGCT**M**ACCATCCA	313 bp	(Loukoianov et al. 2005)	AY747599.1
Ta30797		GCCGTGTCCATGCCAGTG	TTAGCCTGAACCACCTGTGC	126 bp	(Paolacci et al. 2009)	TC279294
TaPAL	phenylalanine ammonia-lyase	GCGGTCTCCTGGCGAAGAGG	GCACACTACTCTTCACTTTCTCGATCC	173 bp		HX081317

Suppl.Table2

Supplemental Table 2.

	1	2	3	4	5	6	7
A		Σ	WHEAT or ARATH 1e-40	WHEAT or ARATH 1e-40 Non-Redundant	Full HEATMAP	Filtered HEATMAP	
	Full datasets	1064	319/1064	200/1064	200/1064	137/1064	
B		Σ	Arabidopsis 1e-40	Arabidopsis 1e-40 Non-Redundant	Gene Ontology Biol. Proc.	Gene Ontology Mol. Funct.	Genes in KEGG Pathways
	D	198	45	29	20	26	14
	G	306	56	49	40	48	21
	D×G-D-G	237	46	29	25	26	9
C		Σ	Arabidopsis annotation	Arabidopsis annotation + TAIR ID	TAIR ID in Network	TAIR ID in Network 1e-40	
	Full datasets	1064	796/1064	790/1064	59/9264	16/9264	